LBL-23888

Lawrence Berkeley Laboratory
UNIVERSITY OF CALIFORNIA

EARTH SCIENCES DIVISION

Interpretation of Shallow Crustal Structure of the Imperial Valley, California, from Seismic Reflection Profiles

L.K. Severson
(M.S. Thesis)

May 1987

Prepared for the U.S. Department of Energy under Contract DE-AC03-76SF00098

DISCLAIMER

LBL--23888

DE88 000472

Interpretation of Shallow Crustal Structure of the Imperial Valley, California, from Seismic Reflection Profiles

Lupe K. Severson
(M.S. Thesis)

Lawrence Berkeley Laboratory
University of California
Berkeley, CA 94720

May 1987

This work was supported by the U.S. Department of Energy
under Contract No. DE-AC03-76SF00098

Interpretation of Shallow Crustal Structure of the Imperial Valley, California, from Seismic Reflection Profiles

Lupe K Severson

Abstract

Eight seismic reflection profiles (285 km total length) from the Imperial Valley, California, were provided to CALCRUST by Exxon USA and Chevron USA for reprocessing and interpretation. Two profiles were located along the western margin of the valley, five profiles were situated along the eastern margin and one traversed the deepest portion of the basin.

These data reveal that the central basin contains a wedge of highly faulted sediments that thins to the east. Most of the faulting is strike-slip but there is evidence for block rotations on the scale of 5 to 10 kilometers within the Brawley Seismic Zone.

These lines provide insight into the nature of the east and west edges of the Imperial Valley. The basement at the northwestern margin of the valley, to the north of the Superstition Hills, has been normal-faulted and blocks of basement material have "calved" into the the trough. A blanket of sediments has been deposited on this margin. To the south of the Superstition Hills and Superstition Mountain, the top of the basement is a detachment surface that dips gently into the basin. This margin is also covered by a thick sequence of sediments.

The basement of the eastern margin consists of metamorphic rocks of the upper plate of the Chocolate Mountain Thrust system underlain by the Orocopia Schist. These rocks dip to the southeast and extend westward to the Sand Hills Fault but do not appear to cross it. Thus, the Sand Hills Fault is interpreted to be the southern extension of the San Andreas Fault. North of the Sand Hills Fault the East Highline Canal seismicity lineament is associated with a strike-slip fault and is probably linked to the Sand Hills Fault.

Although a good picture of the shallow crustal structure of the Imperial Valley was obtained, the use of extended correlation failed to image deep structure. The meta-sedimentary basement is non-reflective and structures deeper than about 4 s (including the Mohorovic Discontinuity) are not seen.

Six geothermal areas crossed by these lines, in agreement with previous studies of geothermal reservoirs, are associated with "faded" zones, Bouguer gravity and heat flow maxima, and with higher seismic velocities than surrounding terranes. The combination of all these characteristics makes a useful tool in the delineation of geothermal reservoirs.

Acknowledgments

There were many people who helped me throughout my sojourn at UC Berkeley. I am grateful to Drs. Thomas V. McEvilly, H. Frank Morrison, and Alex Becker for their assistance and advice in researching and preparing this thesis. Research, of course, is not possible without data so I would like to thank Exxon USA and Chevron USA (Bill Bartling, in particular) for generously providing such a large data set for this study. The seismic data were processed at the Center for Computational Seismology at Lawrence Berkeley Laboratory. Dr. Hiroo Kanamori of CalTech furnished earthquake hypocenter information and discussions with Dick Corbally of the Calif. Div. of Oil and Gas were most helpful.

Dave Okaya could always be counted on to share his DISCO expertise and I appreciated the assistance and encouragement I received from Dr. Norm Goldstein and Dr. Ernie Majer. I am particularly grateful to Dr. Eric Frost for sharing his enthusiasm and knowledge of the Imperial Valley region.

Where would any grad student be without the support, advice, and humor of his/her fellow students? The many discussions and gab sessions I had with Dave Bartel, Jonathon, Jim Nelson, Tom Daley, Dón Vasco, Fred Eastwood, Joel Ita, Cliff, Nick, Tracy, Renee and Ann were invaluable.

Finally, I would like to thank my husband, Roger, for his neverending supply of encouragement and love throughout this endeavor. Without his constant support and help, my road would have seemed endless.

Table of Contents

List of Illustrations

CHAPTER 1
INTRODUCTION

Resolving the tectonic structure and geological history of the southwestern United States is an objective of the California Consortium for Crustal Studies (CALCRUST). To date, the major effort by CALCRUST scientists has gone into the acquisition and interpretation of seismic reflection profiles. This study examines eight seismic reflection lines, located in the Imperial Valley in southeastern California, which were provided to CALCRUST by Chevron USA and Exxon USA.

The Mesozoic and Cenozoic tectonic development of the western United States has been reviewed by many authors (e.g., Atwater, 1970; Coney, 1978; Terres and Crowell, 1979; Zoback *et al.*, 1981). In southeastern California, which was at or near a plate boundary throughout these eras, different tectonic geometries have been overprinted on one another. For most of this time the plate boundary was convergent and crust was accreted and subducted into the North American continent. Compressional tectonics evolved, in mid-Tertiary time, into Basin and Range extension and the San Andreas transform system.

The Salton Trough is a northwest-trending topographic and structural depression which marks the boundary between the Pacific and North American plates in southeastern California (Figure 1). The Imperial Valley, along with the Coachella Valley to the northwest and the Mexicali Valley and Colorado River delta to the southeast, comprise the Salton Trough (Figure 2). Studies of gravity, seismic refraction profiles, seismicity, heat flow, and geology have led to a tectonic model in which the relative shear between the Pacific and North American plates, in this region, is accomodated by a series of *en echelon* spreading centers aligned obliquely to the direction of plate motion (Figure 1) (Atwater, 1970; Biehler *et al.*, 1964; Dibblee, 1954; Elders *et al.*, 1972; Fuis and Schnapp, 1977; Hill *et al.*, 1975; Johnson, 1979; Johnson and Hadley, 1976; Kovach *et al.*, 1962; Larson *et al.*, 1968; Lomnitz *et al.*, 1970). The two northernmost right-stepping spreading centers, where plate motion is transferred to the strike-slip San Andreas fault system, are located in the Imperial and Mexicali

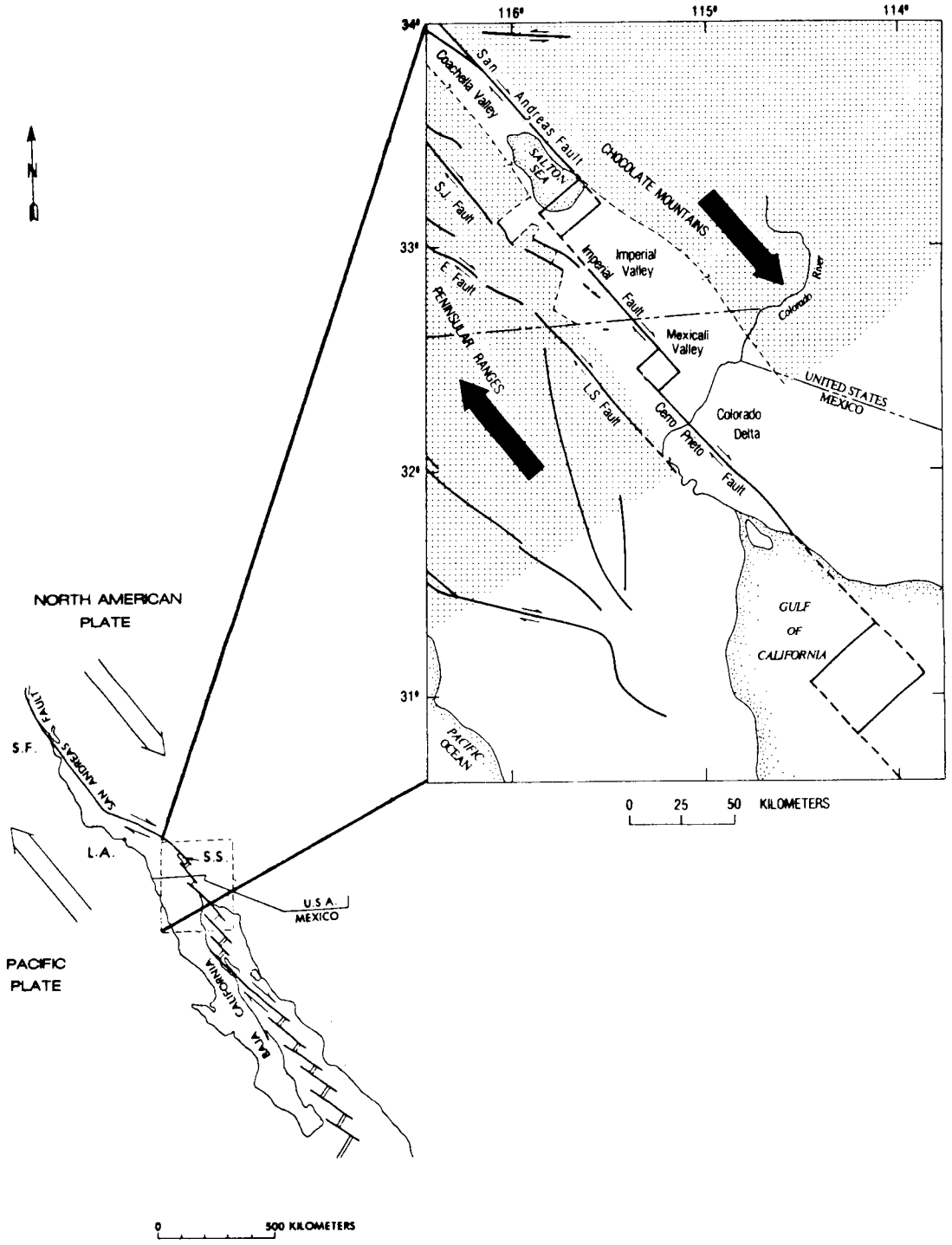

Figure 1. Tectonic map of the Salton Trough adapted from Lachenbruch *et. al.* (1986). Large arrows indicate relative plate motion. Stippled pattern is extent of crystalline basement. Abbreviations are: S.S. = Salton Sea, S.J. = San Jacinto Fault Zone, E. = Elsinore Fault Zone, L.S. = Laguna Salada Fault, L.A. = Los Angeles, S.F. = San Francisco.

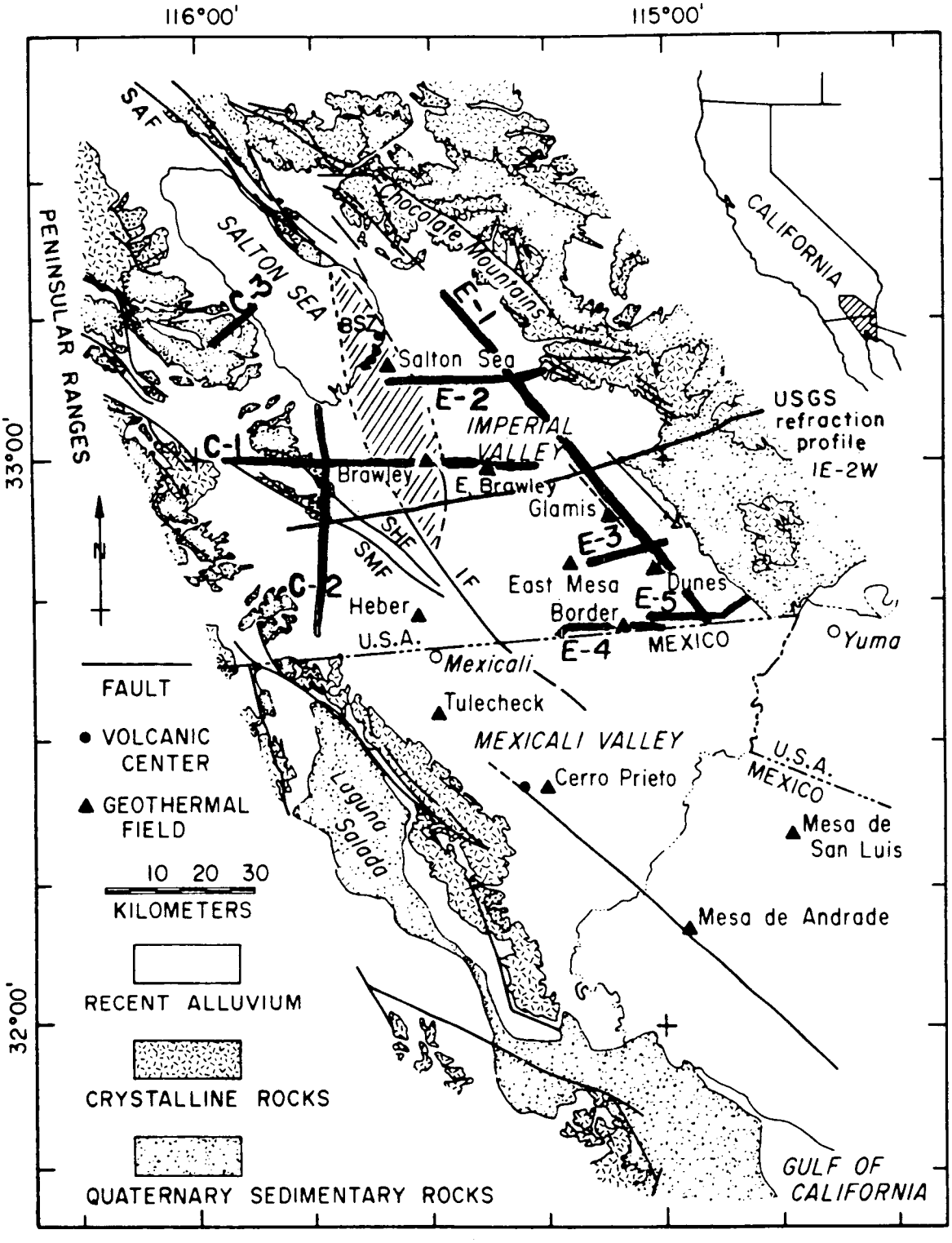

Figure 2. Simplified geologic map of the Imperial Valley region showing locations of seismic reflection profiles. Abbreviations are: BSZ = Brawley Seismic Zone, SHF = Superstition Hills Fault, SMF = Superstition Mountain Fault, IF = Imperial Fault. Modified from Elders and Cohen (1983).

valleys.

Most of the surface in the Imperial Valley region is below sea level. The Salton Sea, located in the topographically lowest portion of the Salton Trough, was formed when the entire flow of the Colorado River was accidentally diverted northwestward during construction on an irrigation project from 1905 to 1907 (Elders, 1979). As would be expected in an area of active continental rifting and transform faulting, the valley is characterized by high heat flow (approx. 140 mW/m^2), frequent earthquakes and earthquake swarms (Lachenbruch *et al.*, 1985; Doser and Kanamori, 1986). Several localized areas of extremely high heat flow (> 200 mW/m^2) have been developed as commercial geothermal energy sources and today there are five power plants, generating 151 MW of electricity, within the valley (Figure 2) (Lachenbruch *et al.*, 1985; DiPippo, 1986). A regional Bouguer gravity high, relative to surrounding terranes, is associated with the Salton Trough (Biehler, 1964). Since the Salton Trough is a basin, filled with up to 16 km of late Tertiary sediments, the anomolously high gravity is attributed to high density mafic intrusives associated with continental rifting (Fuis *et al.*, 1982).

In this study seismic reflection data are used to investigate the nature of the boundary between the Neogene Imperial Valley and the terranes which bound it to the east and west (Figure 2). Seven of the eight seismic reflection profiles studied either cross or run parallel to the edges of the trough. The eighth profile (Line C-1) is an east-west transect of the valley that provides a cross-section of the trough.

The regional geology and tectonic setting of the Imperial Valley region are introduced in Chapter 2. The study area is discussed in three sections: (1) the Imperial Valley proper; (2) the western Imperial Valley and eastern Peninsular Ranges; and, (3) the eastern Imperial Valley and southern Chocolate Mountains. In the central Imperial Valley an inferred spreading center, located between the Imperial and San Andreas faults, is blanketed by up to 16 km of Tertiary sediments (Figure 2) (Fuis *et al.*, 1982). In the western Imperial Valley and the eastern Peninsular Ranges, pre-Cenozoic crystalline rocks associated with the eastern Peninsular Ranges batholith and overlying Cenozoic sedimentary rocks were intensely deformed as shear strain was (and still is)

accommodated by northwest-trending splays of of the San Andreas Fault (the San Jacinto and Elsinore fault zones) (Figure 2) (Sharp, 1982). In contrast, Mesozoic and Proterozoic crystalline rocks, which have been thrust over the Mesozoic Orocopia Schist in the southern Chocolate Mountains, are only slightly deformed by late Tertiary transform tectonics (Figure 2) (Haxel and Dillon, 1978).

Chapter 3 is devoted to a detailed description and discussion of each seismic reflection profile. Lines C-1, C-2, and C-3 of the western Imperial Valley are described first (Figure 2). Lines in the eastern Imperial Valley, E-1 through E-5, are then given similar treatment. Conclusions are presented in Chapter 4.

CHAPTER 2

REGIONAL GEOLOGY AND TECTONIC SETTING

2.1 Imperial Valley

A USGS seismic refraction study of the Imperial Valley region, which also incorporated gravity (Biehler, 1964), heat flow and well data, examined the shallow crustal structure (to 16 km) of the central valley (Figure 2) (Fuis *et al.*, 1982; 1984). The basin is filled with 10 to 16 km of sediments, with the greatest accumulation in the portion of the valley where the inferred spreading center is located. The sediments thin gradually to the east while, to the west, they are truncated by buried scarps which coincide with the Superstition Hills, Superstition Mountain, and Coyote Creek faults (Figure 3). Below 5 or 6 km the sediments undergo a transformation to lower-greenschist-facies metasediments with a seismic velocity of 5.65 km/sec. Fuis *et al.* (1982; 1984) label the metasediments the "basement" and explain the lack of a reflection from the top of the basement as due to a 1 km thick "transition zone" (5.0-5.65 km/sec). Under the metasedimentary basement, a lower crust "sub-basement" consisting of a mafic intrusive complex is inferred from a seismic velocity of 7.2 km/sec, an anomalous gravity high, and the presence of basaltic sills and dikes in some wells (Figure 3). (Fuis and Kohler, 1984; Fuis *et al.*, 1984). The thickness of the "sub-basement" was not determined seismically in the USGS study but the Mohorovic Discontinuity is estimated from gravity data to be from 21 to 23 km deep (Biehler, 1964; Fuis *et al.*, 1982).

The Imperial Valley is the site of frequent earthquakes and earthquake swarms (Johnson and Hill, 1982). It is cut by two major northwest-trending, right-lateral, strike-slip faults (Figures 1 and 2). The more northerly of the two is the San Andreas Fault while to the south is the Imperial Fault. The southeast end of the San Andreas Fault is linked to the northwest end of the Imperial Fault by a band of seismicity called the Brawley Seismic Zone. The coincidence of this zone with areas of high heat flow and with several Quaternary volcanic domes has led to the conclusion that a

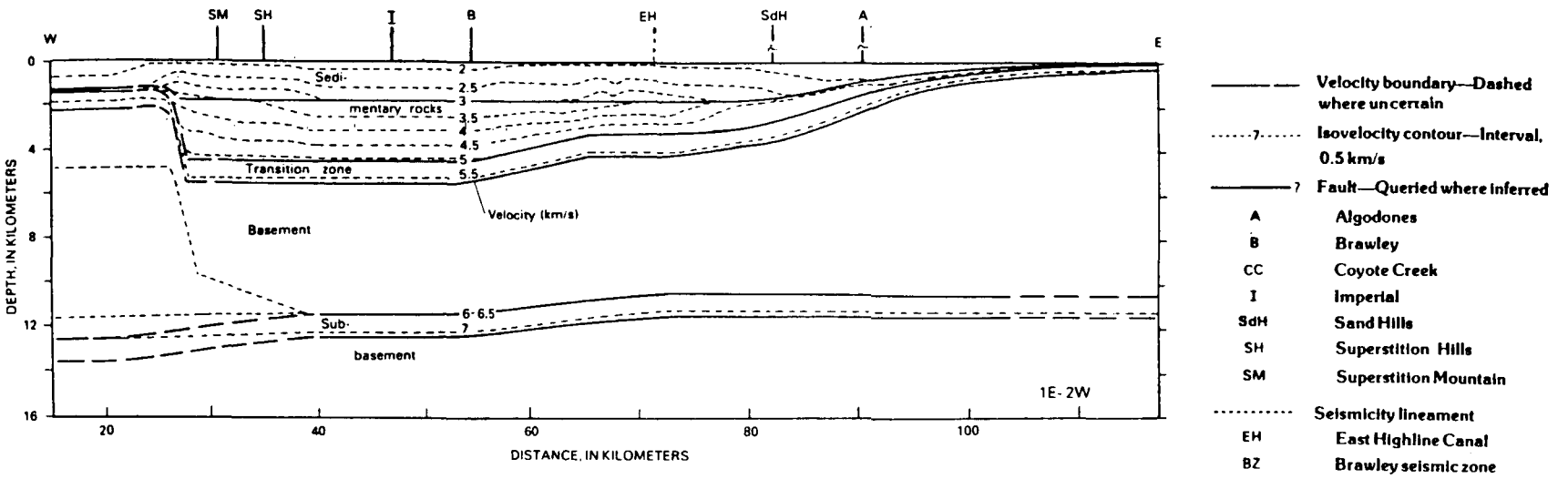

Figure 3. Seismic refraction profile 1E-2W, adapted from Fuis *et al.*, (1982; 1984), with interpretation of velocity and geologic stucture of the Imperial Valley. See Figure 2 for location.

spreading-center exists in the continental crust below (Figure 1) (Biehler *et al.*, 1964; Elders *et al.*, 1972; Larson *et al.*, 1968; Lomnitz *et al.*, 1970).

2.2 Western Imperial Valley and Eastern Peninsular Ranges

The late Tertiary Salton Trough is the northward, nonmarine extension of the Gulf of California (Elders *et al.*, 1972; Larson *et al.*, 1968; Lomnitz *et al.*, 1970). Early sediments in the trough consisted of deltaic and marine deposits. Marine sedimentation ceased when southwest progradation of the Colorado River delta separated the trough from the Gulf of California in Pliocene time (Winker, 1987). After that time, intermittent inundations by the river kept sedimentation rates approximately equal to subsidence rates and, thus, maintained surface elevations near sea level. (Dibblee 1954, 1984; Sharp 1972).

The Cenozoic stratigraphy of the Salton Trough is well exposed in the western Imperial Valley (Figure 4) (Dibblee, 1954; 1984; Winker, 1987). The Miocene Split Mountain Formation, a nonmarine sequence of conglomeratic sandstones and fanglomerates, rests unconformably on pre-Cenozoic crystalline rocks (Figure 4) (Dibblee, 1954; 1984; Johnson *et al.*, 1983; Gibson *et al.*, 1984; Sharp, 1972; Winker, 1987). Interbedded with the Split Mountain Formation are basalt flows of the Alverson Formation and the Fish Creek Gypsum (Sharp, 1982). Deposited on the Split Mountain Formation are the the sands, silts and clays of the Mio-Pliocene Imperial Formation which represent a change from terrestrial to marine sedimentation. The overlying sands and clays of the Palm Spring Formation, representing deltaic, lacustrine, and brackish depositional environments, grade laterally to the north into the Canebrake Conglomerate (Johnson *et al.*, 1983; Gibson *et al.*, 1984). The youngest rock units identified in the Imperial Valley, the Borrego Formation, Ocotillo Conglomerate and Brawley Formation, represent a transition from lacustrine to terrestrial and then back to a lacustrine environment in Pleistocene time (Dibblee, 1984). These Neogene sedimentary rocks are inferred to lie at depth in the central Imperial Valley but, to date, no well has verified this (Figure 3) (Dibblee, 1984; Sharp, 1972).

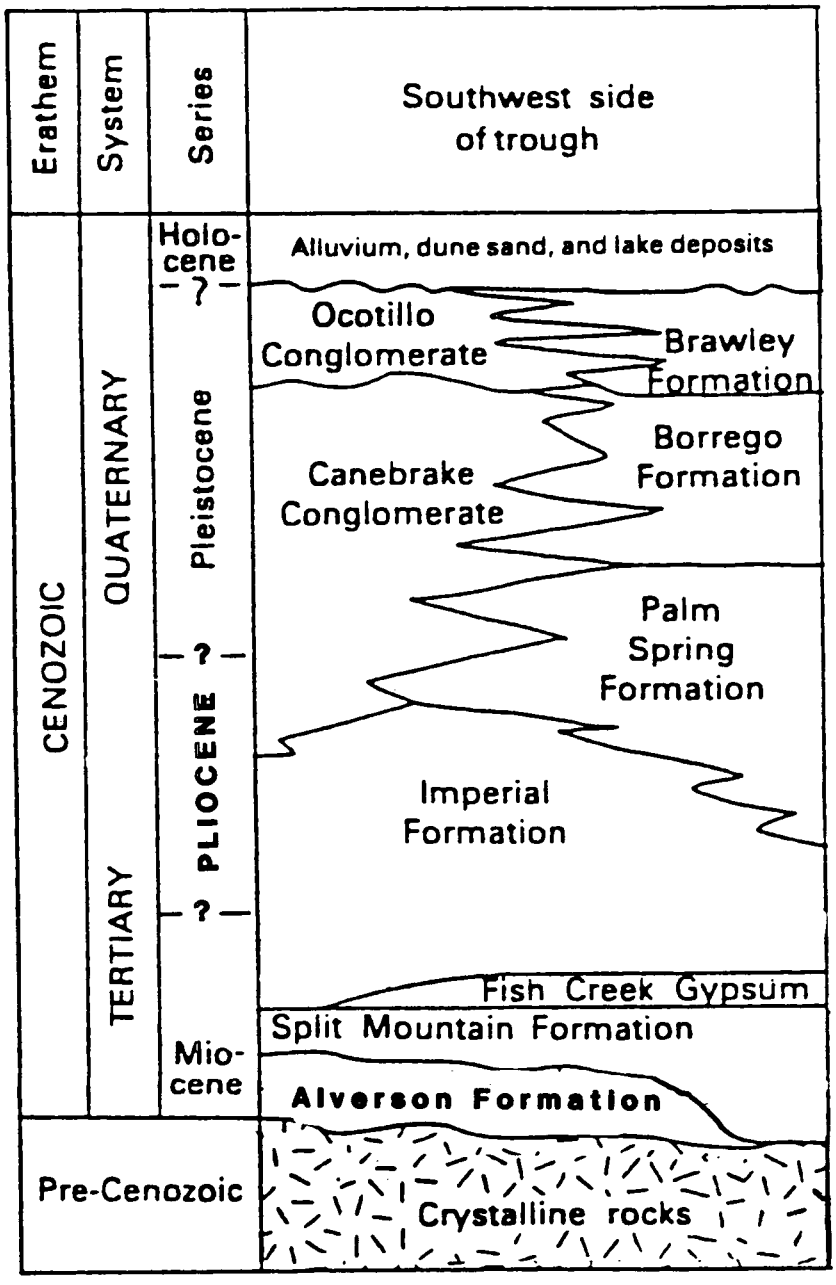

Figure 4. Composite Cenozoic stratigraphic column of the western Imperial Valley. Modified from Sharp (1982) after Winker (1987).

In the western Imperial Valley the sedimentary rocks rest on a platform of pre-Cenozoic crystalline rocks (Dibblee, 1954). These crystalline rocks consist of metasedimentary and metavolcanic country rocks in which the mid-Cretaceous granites of the southern California batholith were emplaced (Sharp, 1982). The metamorphic rocks consist of mid-Cretaceous age banded gneisses, quartzites, marbles and mica schists. A zone of mylonitic fabric, prevalent throughout the area in the granitic rocks, is called the Santa Rosa mylonite zone (Sharp, 1967; Wallace and English, 1982). This zone consists of rocks ranging from augen gneiss to ultramylonite (Sylvester and Bonkowski, 1979). Mylonitization occured prior to approximately 63 m.y.B.P. and is associated with mid-Cretaceous to early Cenozoic thrust faulting (Sharp, 1979; Wallace and English, 1982).

Several major Tertiary faults, over which the right-lateral slip of the San Andreas Fault system is regionally distributed, are responsible for the segmentation, rotation, and transpressive deformation of both Cenozoic and pre-Cenozoic rocks (Figure 5). The northwest-trending Clark Valley, Coyote Creek, Superstition Hills, and Superstition Mountain right-lateral strike-slip faults are all components of the San Jacinto Fault Zone. To the south is the Elsinore Fault Zone which also consists of several northwest-trending, right-lateral strike-slip fault strands. Historical earthquakes and ground displacement have been associated with a number of these faults (Sharp, 1982; Doser and Kanamori, 1986).

The Superstition Hills are a northwest-trending anticlinal structure located mostly north of the Superstition Hills Fault (Figure 5). They consist of low badlands eroded from the poorly indurated, highly deformed Brawley Formation (Dibblee, 1984). Superstition Mountain, easily confused with Superstition Hills but located to their south (Figure 5), consists of pre-Cenozoic granitic intrusive rocks, the Borrego, Alverson and Split Mountain Formations unconformably overlain by the Ocotillo Conglomerate and the Brawley Formation (Dibblee, 1984; Winker, 1987). To the southeast of Superstition Mountain, along the trace of the Superstition Mountain Fault, outcrops of the Borrego Formation, Ocotillo Conglomerate, and Brawley Formation are deformed into tight,

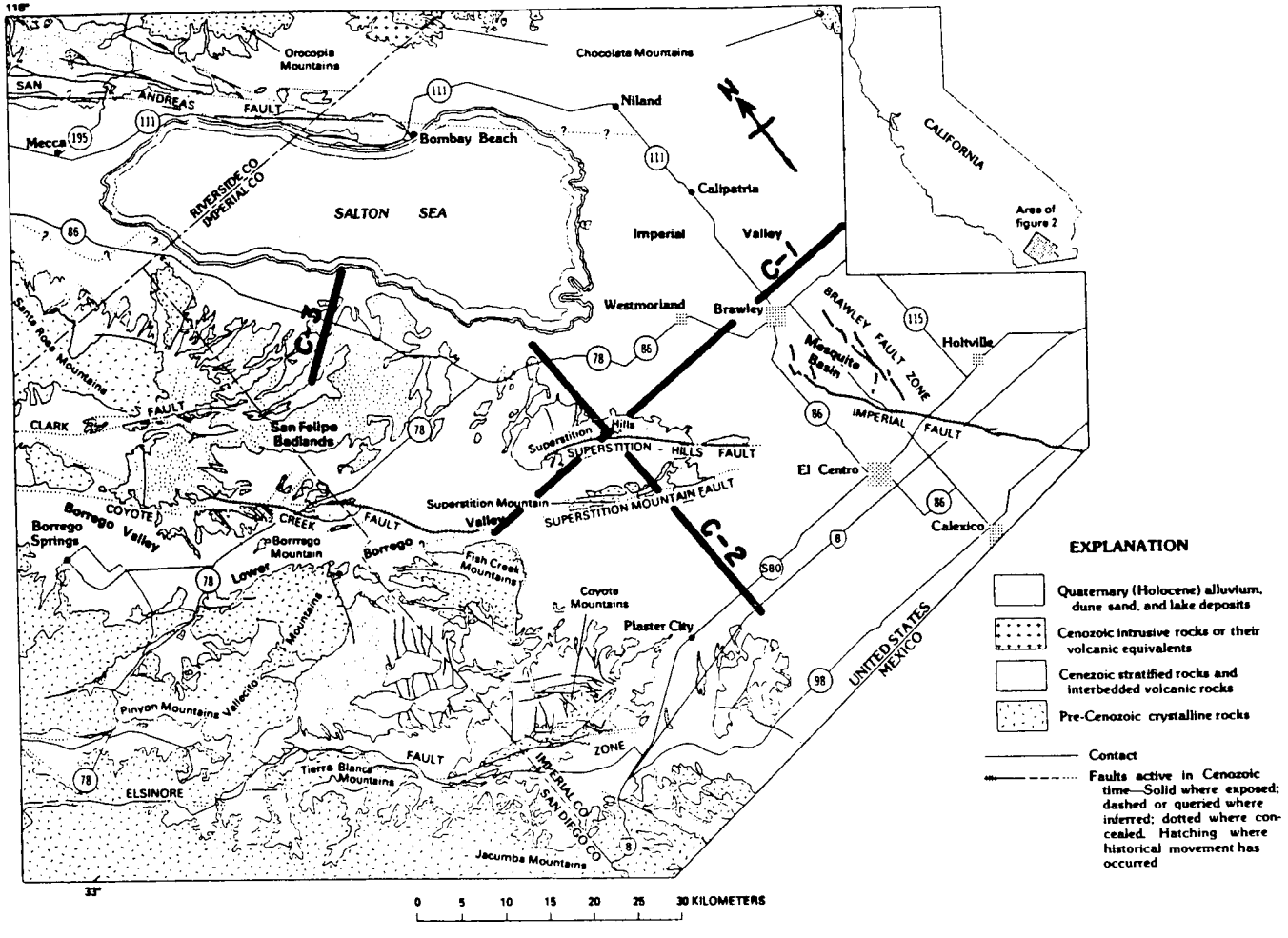

Figure 5. Generalized geologic map of the western Imperial Valley modified from Sharp (1982).

east-trending folds (Figure 5) (Dibblee, 1984). East-trending drag folds indicate right-lateral movement on the Superstition Hills and Superstition Mountain Faults (Dibblee, 1954) Although, slip has not been observed in historic time, some seismicity has been associated with the Superstition Mountain Fault (Sharp, 1982; Doser and Kanamori, 1986). In contrast, historic displacements have repeatedly occurred on the northerly Superstition Hills Fault (e.g. Allen *et al.*, 1965; Fuis, 1982; Sharp *et al.*, 1986).

Recent field work in the western Imperial Valley and southern Santa Rosa Mountains has identified the existence of low-angle normal (detachment) faulting which appears to be regional in extent (Wallace and English, 1982; Engel and Schultejahn, 1984; Frost, pers. comm. 1987). The age of detachment faulting is mid-Tertiary. In places, faults occur where Mesozoic, rigid mylonite zones are in contact with Tertiary, soft upper-plate sediments forming propitious planes for fault propagation. Along strike, faulting, at a deeper level, juxtaposes granitic rocks and is identifiable by a zone of brecciation and hydrothermal alteration (Wallace and English, 1982). The undulating regional detachment surface generally dips to the northeast and is cut and displaced by strike-slip faults of the San Andreas system.

2.3 Eastern Imperial Valley and Southern Chocolate Mountains

Broadly speaking, the southern Chocolate Mountains, which form the eastern border of the Imperial Valley, consist of Mesozoic and Proterozoic rocks thrust to the northeast over the late Mesozoic Orocopia Schist by the Chocolate Mountain Thrust (Figure 6) (Dillon, 1976; Haxel and Dillon, 1978; Haxel *et al.*, 1985; 1986). Mylonite and other cataclastic rocks are associated with the thrust zone throughout the Chocolate Mountains (Crowell, 1981). Upper-plate rocks consist mostly of Proterozoic granites and gneisses and Mesozoic granites. Recently, a Jurassic(?) age unit, the Winterhaven Formation has been identified in the upper-plate (Haxel *et al.*, 1985). This formation is predominantly argillitic siltstone, silty argillite, and graywacke and is interbedded at its base with Early to Mid-Jurassic metavolcanics. In some locations, the Winterhaven Formation has been moved by Late Cretaceous low-angle faulting into contact with the

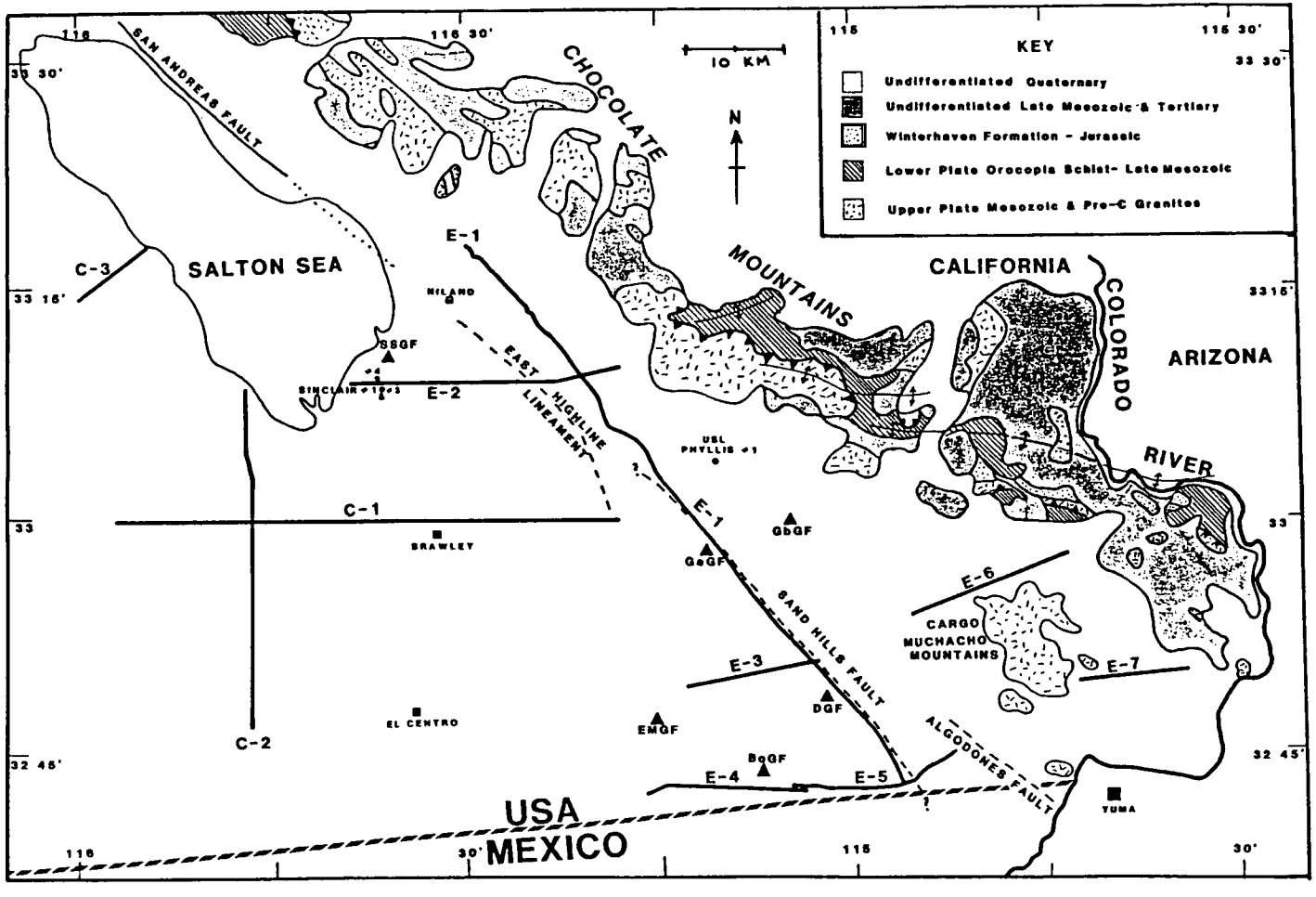

Figure 6. Generalized geologic map of the eastern Imperial Valley. Geothermal field abbreviations are: SSGF = Salton Sea, Ga = east Glamis, Gb = west Glamis, EM = East Mesa, D = Dunes, Bo = Border. Geology based on Murray *et al.*, (1980).

Orocopia Schist (Haxel *et al.*, 1986). The lower-plate consists of the Orocopia Schist and is predominantly quartzofeldspathic schist derived from sandstone with minor ferromanganiferous metachert, marble, metabasalt, and minor meta-ultramafic rocks (Haxel and Dillon, 1978; Tosdal, 1982; Haxel *et al.*, 1986). The age of movement on the Chocolate Mountains Thrust and metamorphism of the Orocopia Schist are synchronous. Both occurred between about 87 to 74 m.y. ago (Haxel *et al.*, 1986).

Extensive mid-Tertiary calc-alkaline plutonic and volcanic rocks unconformably overlie both upper and lower-plate rocks. These siliceous igneous rocks are in turn unconformably overlain by middle to late Miocene fanglomerates and interebedded basalt flows. The youngest rocks are the early Pliocene marine Bouse Formation and Plio-Pleistocene alluvial sediments (Wilkinson and Wendt, 1986).

The Cargo Muchacho Mountains, in southeasternmost California (Figure 6), are composed of upper-plate mafic to intermediate orthogneisses with granitic intrusions (Wilkinson and Wendt, 1986). The Chocolate Mountains Thrust is not exposed in this location.

Mesozoic compression and mid-Tertiary extension affected most of the Colorado River region. In southeastern California, deformation from these tectonic episodes is overprinted by Mio-Pliocene transform faulting. The regional topography is largely due to the folding of a mid-Tertiary detachment fault surface (Frost *et al.*, 1982). The southern Chocolate Mountains are formed by a northwest-trending anticlinorium (Haxel *et al.*, 1985). Locally within the Chocolate Mountains, tilted Tertiary rocks are separated from pre-Tertiary rocks by detachment faults. The Chocolate Mountains Thrust is in some places cut by detachment faulting, and in others detachment faulting appears to have reactivated some portions of the thrust (Frost *et al.*, 1982; Haxel and Grubensky, 1984).

The Chocolate Mountains area has little recent seismic activity. A small number of earthquakes are associated with the East Highline Canal Seismicity Lineament (Figure 6) (Fuis *et al.*, 1982; Doser and Kanamori, 1986).

CHAPTER 3
SEISMIC DATA DESCRIPTION AND DISCUSSION

3.1 Data Acquisition and Processing

The seismic reflection profiles in this study were acquired by Chevron USA and Exxon USA in the years from 1970 to 1973 and were donated to CALCRUST for use in their crustal studies (Figure 2). Table 1 contains a summary of pertinent facts about each profile.

Table 1. Summary of seismic reflection lines.

Profile	donated by	seismic source	field tapes available	trace length (s)	line length (km)	line direction
Line C-1	Chevron	dynamite	yes	4.7	64	E-W
Line C-2	Chevron	dynamite	no	4.8	40	N-S
Line C-3	Chevron	Vibroseis	yes	11	11	NW-SE
Line E-1	Exxon	Vibroseis	no	4	83	NE-SW
Line E-2	Exxon	Vibroseis	yes	13	32	E-W
Line E-3	Exxon	Vibroseis	yes	13	16	NW-SE
Line E-4	Exxon	Vibroseis	no	4	17	E-W
Line E-5	Exxon	Vibroseis	no	4	22	E-W

Lines for which field tapes were available, Lines C-1, C-3, E-2, and E-3, were completely reprocessed from initial field gathers to stacked CDP sections. The basic processing sequence included extended correlation of the Vibroseis (Trademark, CONOCO Inc.) lines, velocity analysis, automatic gain control (AGC) with a 2 s window, muting, bandpass filtering, stacking, and wave equation migration. Tapes of stacked CDP sections, processed by Chevron USA and Exxon USA, were provided for Lines E-1, E-4, and E-5. The only reprocessing performed on these lines was wave equation migration. There were no field or stack tapes available for Line C-2 but a film copy of the stacked CDP section was furnished so that reproduction and interpretation were possible.

The algorithm used to migrate the stacked sections was a finite-difference approximation to the wave equation. The lines which were totally reprocessed were migrated using smoothed, scaled (80%), stacking velocities. A velocity of 2 km/s, selected based on constant velocity migration tests, was used to migrate the other lines. Extended correlation is a method whereby standard industry reflection data may be processed to greater travel times by re-correlating the field gathers with a shortened sweep (Okaya, 1986). Lines E-2, E-3, and C-3 were suitable for this method. Any other specialized techniques that were applied to any specific line are explained in the section devoted to that line. In general, the Vibroseis shot gathers were plagued by a prevalent source noise problem (Figure 7). After much testing, including f-k filtering severe muting proved the most effective way of alleviating the effect of the noise. All of the lines in the study were referenced to a datum of sea level.

3.2 Western Imperial Valley

3.2.1 Line C-1

Line C-1 is a 62 km east-west transect of the Imperial Valley (Figure 5) shot in 1970 using dynamite as a seismic source. 48-channel shots with split-spread geometry were recorded for a length of 6 s at 268.2 m (880 ft) intervals. Geophones were spaced at 67.1 m (220 ft) intervals. Sub-surface coverage varied from 600% to 1200%. The general processing sequence was as previously described except that surface-consistent residual statics were computed and applied. A 40 ms deconvolution operator was used before stacking to eliminate reverberations in some of the shots. Field tapes were unavailable for the far western portion of the line (kilometers 55 to 62) but a copy of the Chevron-processed, un-migrated, stack was spliced onto the data processed by CALCRUST.

Line C-1 provides a good picture of the shallow crustal structure of the eastern Imperial Valley that complements the model proposed by Fuis *et al.* (1982) (Plate 1). The predicted tapering of the sedimentary section to the east, is evident by the general

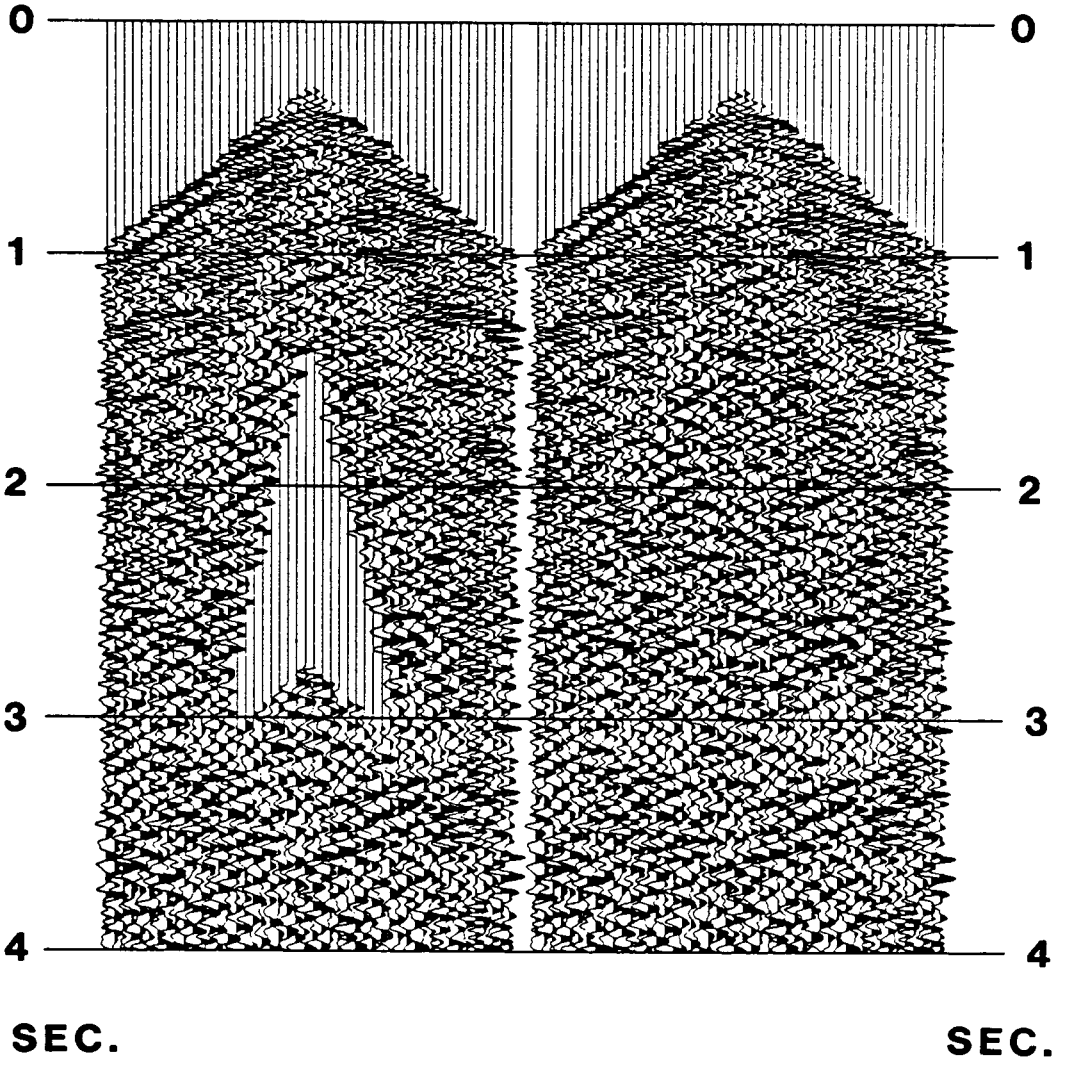

Figure 7. Representative shot gather illustrating a pervasive air-wave problem which plagued all of the reflection profiles in this study. The effect of the air-wave was alleviated by the mute shown. This is shot 75 from Line C-3.

west-dipping nature of reflections in the eastern portion of the stacked section. This sedimentary wedge is far from homogeneous. Sediments in the central Imperial basin since Pliocene time consist of deltaic deposits of the Colorado River interfingered with lacustrine muds and silts and sediments derived from the basin edges (Winker, 1987). This laterally discontinuous style of sedimentation is evident in Line C-1. Reflectors cannot be traced for more than one or two kilometers before they disappear or are truncated by one of the numerous steeply-dipping to vertical faults which dissect the near-surface sediments.

Strike-slip is the principal mode of faulting in Line C-1 as deduced from the association of flower or palm structures with faults (Plate 1). D'Onfro and Glagola (1983) include flower structures in a list of criteria for identifying wrench faults in a single seismic section. The upward-branching of the faults at kilometers 25 and 30 illustrates how the terms "flower" and "palm" structure originated. The other criteria (e.g. abrupt dip changes across faults) involve changes in seismic character resulting from viewing a cross-section of two blocks which have been displaced, relative to each other, either into or out of the plane of the section. This juxtapostion of different strata across strike-slip faults in Line C-1 is probably a factor which contributes to the previously described lateral heterogeneity of the sediments.

The abrupt change in dip across the fault at kilometer 28 could be indicative of the northward (or southward) translation of the blocks to either side of it. Strike-slip movement may have placed blocks with differing stratigraphy next to each other. Very slight growth fabric may be shown by the segments on either side of the fault, as well as the segment from kilometers 21 to 24, which would indicate syndepositional deformation. This suggests that dip-slip could be involved in the fault movement. Another explanation for the dips seen in the blocks from kilometers 26 to 29 and 21 to 24 is that they are the result of deformation related to block rotation.

Many authors, on the basis of geologic field relations, paleomagnetic measurements and seismicity studies, have suggested that the style of tectonism between strike-slip faults is one of crustal blocks accomodating right or left-lateral slip by

rotation (e.g. Cox, 1980; Luyendyk *et al.*, 1980; Ron *et al.*, 1984). A geometrical model of block rotation in the San Andreas Fault system, as described by Nicholson *et al.* (1986), requires the clockwise movement of blocks on shallow crustal detachment surfaces. They postulate that segmentation of the crust occurs between parallel sets of northwest-trending, right-lateral faults and northeast-trending, left-lateral faults. Deformation of the rocks in a block occurs as the corners of the block rotate into or away from the bounding fault planes. Block rotations in a strike-slip environment occur at scales ranging from a few centimeters to several kilometers (Figure 8).

The blocks under discussion, from kilometers 21 to 24 and 26 to 29, are located within the Brawley Seismic Zone, the zone of seismicity associated with the inferred spreading center joining the strike-slip Imperial and San Andreas Faults (Figure 2). Johnson and Hadley (1976) and Nicholson *et al.* (1986) delineated northeast-trending, left-lateral faults within this zone based on seismicity and earthquake source mechanism studies which, unfortunately, do not intersect Line C-1. Thus, block rotations as a cause of deformation from kilometers 21 to 29 are postulated but the geometry of the three-dimensional blocks (i.e. the location of the bounding faults) is unknown. A study of earthquake source mechanisms would be a means of verifying this hypothesis.

Of the faults which intersect Line C-1 only the Brawley Fault (kilometer 19) and Superstition Hills Fault (kilometer 46) have mappable surface expression in the vicinity of the seismic line (Figure 5). The East Highline Canal seismicity lineament (Figure 6) (kilometer 2), as outlined by Fuis and Kohler (1984), coincides, in the seismic section, with a vertical fault which separates sediments that differ in reflective character indicating strike-slip motion. Thus, this lineament may represent the southerly extension of the San Andreas Fault. The implications of this will be discussed in more detail in Section 3.3.2 where Line E-2, which also intersects the East Highline Canal seismicity lineament, is discussed.

A fault located at kilometer 58 can be correlated with the northwestward projection (towards the Coyote Creek Fault) of the Superstition Mountain Fault (Figure 5). This correlation is highly speculative since this fault has not been active since late

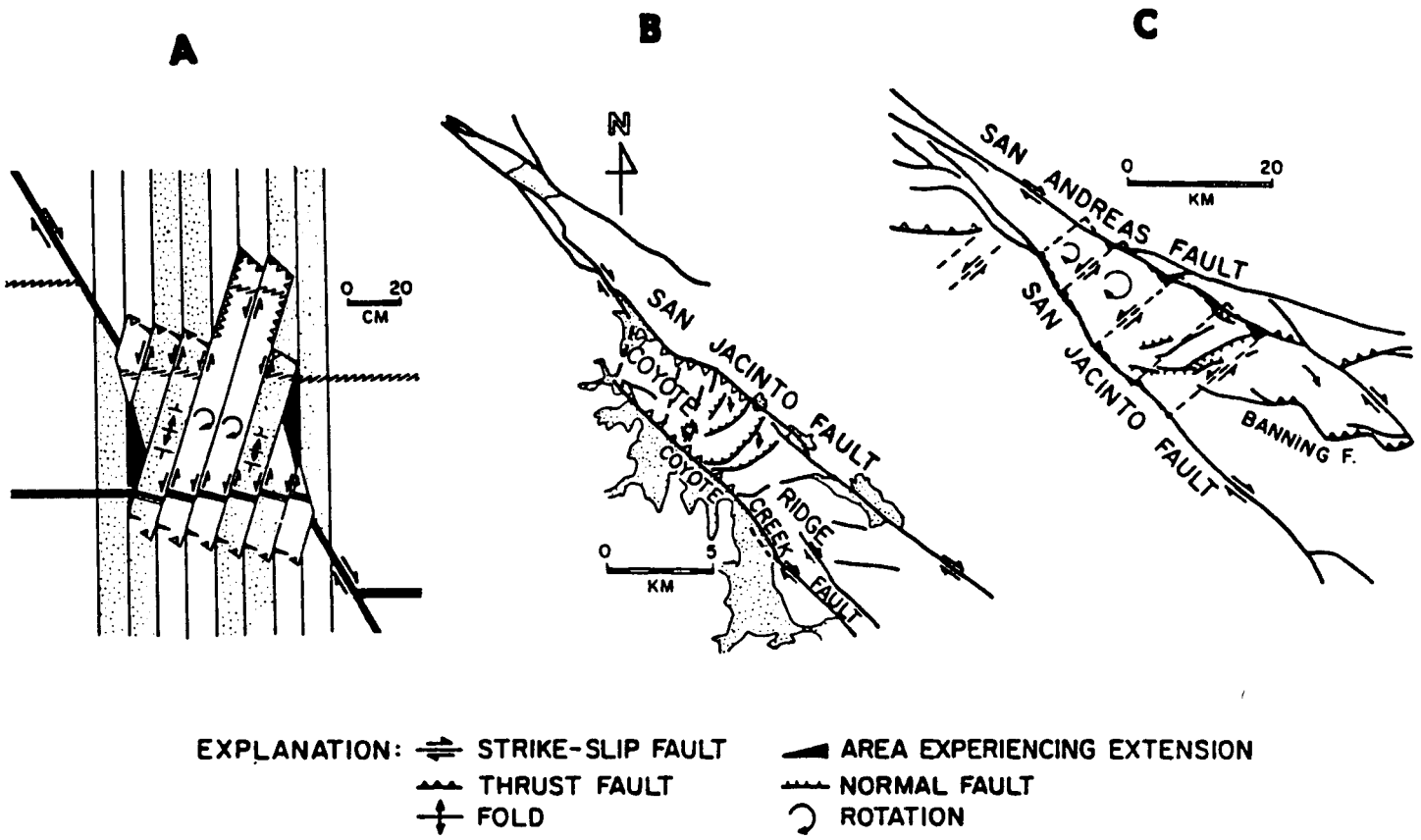

Figure 8. Geologic examples of block rotations by strike-slip faulting on scales from millimeters to kilometers. (A) Rotation of a hard surface layer controlled by evenly-spaced plowed furrows (ruled lines) from the 1979 Imperial valley earthquake. (B) Rotating blocks between the Coyote Creek and San Jacinto faults. (C) Block model for shear rotation near the intersection of the San Jacinto and San Andreas faults. Directly from Nicholson *et al.*, (1986).

Pleistocene (Dibblee, 1984) and the mappable trace of the fault is located several kilometers to the southeast.

The Superstition Hills Fault (kilometer 46), which is traceable on the surface to within a zone 2 m wide (Sharp *et al.*, 1986), is obscured in the seismic section by the lack of coherent reflections from the folded rocks of the Superstition Hills. The Superstition Hills formed by uplift and compression at the restraining bend created by the fault as it curves to the west. They consist of low badlands eroded from the folded, poorly indurated, late Pleistocene Brawley Formation. These conditions are not favorable for the transmission of seismic energy and it is not surprising that the Superstition Hills are associated with a zone of poor reflectance. There may also be interference from the fault plane itself since the fault intersects Line C-1 at an angle of about 45° and then curves west until it almost parallels the line.

Across Line C-1 coherent reflections are observable only to a maximum time of about 3 s. From the extensive refraction study conducted by the USGS (Fuis *et al.*, 1982), two kinds of basement are expected to be present in Line C-1. To the east of the Superstition Hills Fault, the basement consists of sediments metamorphosed to lower-greenschist-facies. To the west, the basement is granitic intrusive rock (Dibblee, 1984). The transition from metasedimentary to crystalline basement, which occurs at a steep scarp that coincides with the Superstition Hills Fault (Fuis *et al.*, 1982), is not imaged in the seismic section.

Using the velocity structure from Profile 1E-2W of the USGS refraction study (Figure 2) and a basement depth map developed from the same study (Figure 9) (Fuis and Kohler, 1984), the two-way travel time to the top of the basement was calculated and then plotted on the seismic section (Plate 1). As was found in the USGS refraction study, there is a lack of a discernible reflection from the top of the "metasedimentary" basement. The same is true for the crystalline basement. The calculated basement contour, across the entire seismic section, roughly corresponds to the deepest time at which coherent reflectors are visible. The lack of reflectors within the metasedimentary basement is probably due to poor penetration of seismic energy through young,

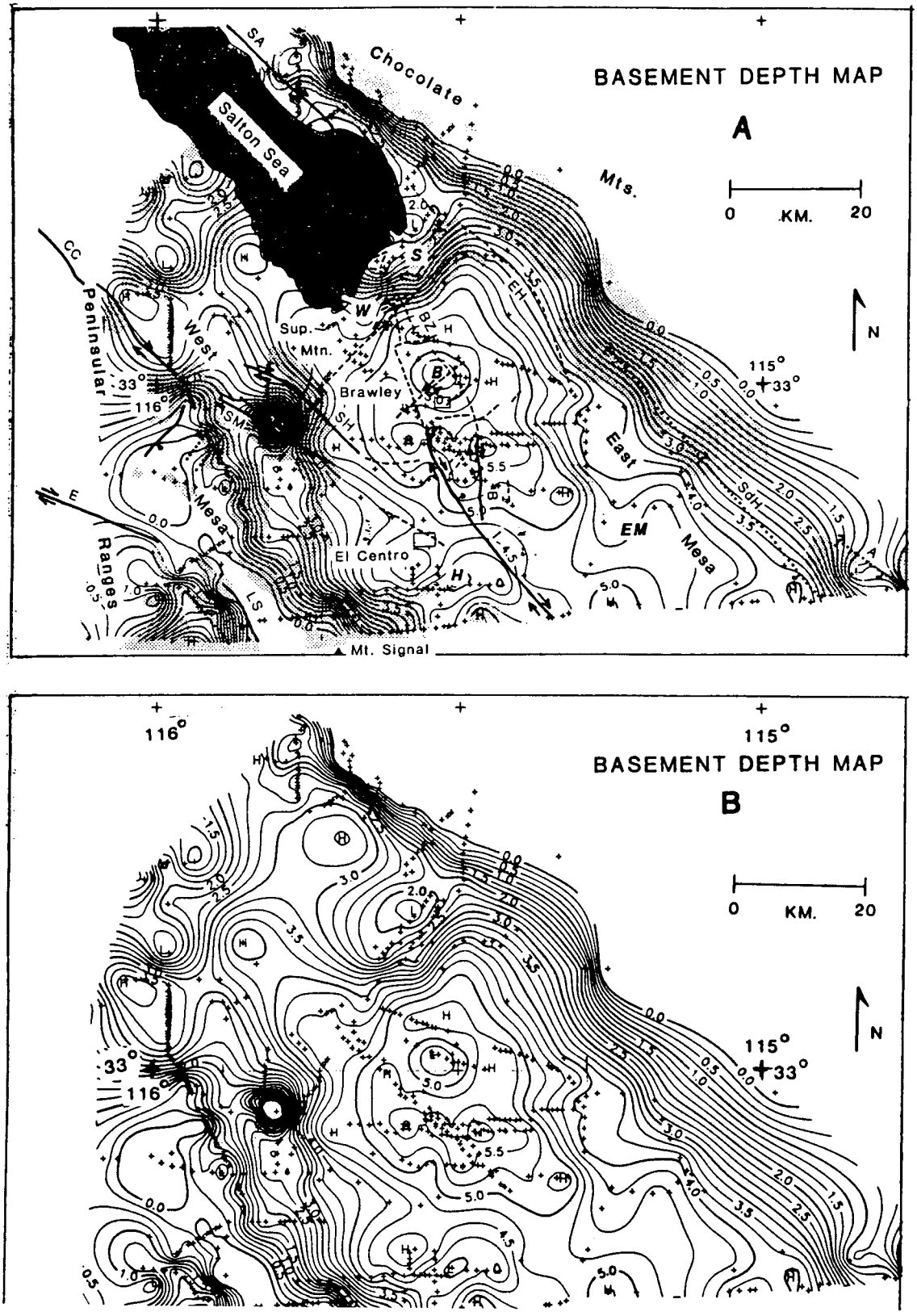

Figure 9. Basement depth map of the Imperial Valley directly from Fuis and Kohler (1984). Numbers are depths (in km) to material with velocity greater than 5.6 km/s. Contour interval is .25 km. +'s are station-data points.

inhomogeneous sediments and, also, due to sediment alteration associated with increasing thermal metamorphism with depth.

Relocated hypocenter depths from 71 earthquakes, recorded by the California Institute of Technology array from 1977 to 1983, were also converted to two-way travel time using a smoothed velocity model obtained from Fuis *et al.*, 1982 (Doser and Kanamori, 1986). The hypocenters, ranging in depth from 7 to 10 km, lie below the basement contour from 3.8 to 4.8 s (kilometers 19 to 30) (Plate 1). At the surface, the region defined by these and thousands of other earthquakes is called the Brawley Seismic Zone. (Several earthquakes were located in the Superstition Hills and three earthquakes define the East Highline Canal seismicity lineament). The hypocenters all occur within the non-reflective basement. This indicates that, although they are not imaged at these depths, some of the faults in the shallow sediments probably extend into the basement.

Line C-1 provides an opportunity to examine the seismic expression of two geothermal fields, the East Brawley (kilometers 0 to 11) and the Brawley (kilometers 19 to 25) (Plate 1). There is little public information available from these areas but it is known that deep wells drilled in these fields penetrated the sediments to depths of 3 to 4 km and recorded temperatures of 200° C at these depths (Brook and Mase, 1981; Elders, 1979; Muffler and White, 1969). Wilson #1 (kilometer 15), total depth 4,097 m and located 10 km south of Line C-1, encountered hot brine at about 4 km depth. Borchard A-1 and A-3 (kilometers 2.5 and 4.5, respectively) produce hot brine from intervals between 3 to 4 km in the East Brawley geothermal field (Brook and Mase, 1981). The top of the reservoir at the Brawley geothermal field is estimated to be at 1.5 km (or 1.3 s using the earthquake hypocenter relocation velocity model) (White and Williams, 1975). Increased permeability from fractures created by thermal recrystallization at these depths accounts for the presence of the hydrothermal zones. A high chlorite presence beginning at about 2 km depth (1.6 s) suggests that low-grade greenschist-facies metamorphism is occurring there (Brook and Mase, 1981). The increased density that results from the cementation, recrystallization, thermal and

hydrothermal metamorphism of the sedimentary rocks is reflected in a Bouguer gravity maximum over the Brawley and East Brawley fields (Plate 1) (Biehler, 1964; Elders, 1979). Gravity maximums are also associated with the other geothermal areas in the Imperial Valley (Figure 2). Mafic dikes penetrated by wells in the Salton Sea, Heber, and East Brawley geothermal fields, indicate that intrusive igneous rocks could also be a source of excess mass (Robinson *et al.*, 1975; Elders, 1979; Keskinen and Sternfeld, 1982).

Seismic reflection studies conducted elsewhere in the Salton Trough, in the Cerro Prieto and East Mesa geothermal fields (Figure 2), noted the coincidence of a poorly reflective zone (PRZ) with geothermal reservoirs (Blakeslee, 1984; van de Kamp *et al.*, 1978). A zone of poor reflectivity within the producing zones is exhibited in Line C-1 at both the Brawley and East Brawley geothermal fields (Plate 1). Both Cerro Prieto and East Mesa studies observed that the PRZ corresponded to regions of increased seismic velocities. This is true for the Brawley and East Brawley fields, also. Smoothed stacking velocities show a slight increase within these areas relative to the rest of the line (Plate 1). The increased velocities and poor reflective quality associated with geothermal reservoirs is probably due to sediment alteration as discussed previously.

In Plate 1 the correlation of gravity and velocity highs, and poor reflectivity zones with the geothermal fields is immediately apparent. A lack of reflectivity is hardly unusual but when combined with other measurements it can be useful in geothermal reservoir delineation.

3.2.2 Line C-2

Line C-2 extends in a north-south direction from the southern tip of the Salton Sea for 40 km (Figure 5). It passes through the Superstition Hills, Superstition Mountain, and terminates at Yuha Buttes. The Yuha Buttes consist of the Alverson, Split Mountain, Imperial, and Palm Spring Formations bounded to the south by northwest-trending right-lateral faults of the Elsinore Fault System (Dibblee, 1954).

Only a film copy of the stacked CDP section was available for this study so reprocessing of this line was not possible (Figure 10). The data, collected in 1970, consist of 48-channel, split-spread shots recorded for 6 s. Shots at 268.2 m (880 ft) intervals were recorded into groups spaced every 67.1 m (220 ft). However, the copy of the stacked section provided extends to only 4.8 s. Subsurface coverage is 6-fold. Chevron processing included deconvolution with an 80 ms operator and the calculation and application of residual statics.

One of the most striking features on this line is the undulating, high amplitude reflector from kilometers 25 to 35 at about 1.3 to 1.6 s (Figure 10). This reflector occurs where the line crosses the east flank of a -40 mgal Bouguer gravity high (kilometers 29 to 35) (Biehler, 1964). The gravity decreases only slightly to the south before it starts increasing again as it approaches another maximum (-30 mgal) at Yuha Buttes. The gravity increase plus the diffraction at kilometer 36 supports the interpretation that a fault disrupts the high amplitude reflector, dropping it down to the north. Texaco F.D. Browne #1, a well drilled to 2379 m depth, 670 m east of Line C-2 (kilometer 37.5), penetrated altered granite at 2360 m. Therefore, this strong reflector is interpreted as the top of crystalline basement. The sediments above the basement are in angular discordance with it. These north-dipping sediments could represent sloping alluvial fan deposits or the sediments could be in fault contact with the basement and their dipping nature is the result of fault movement.

The brief core descriptions from the botton 3.7 m of F.D. Browne #1 indicate that the basement contact is indeed a fault. They describe reworked, .64 cm (1/4 inch), angular granite pebbles, mottled light gray in color, in an identical matrix with streaks and patches of bronze micas and possible bright green chlorites (California Division of Oil and Gas, 1952). This description is similar to a description of lower-plate rocks from mid-Tertiary low-angle normal (detachment) faults in the southern Santa Rosa Mountains (Wallace and English, 1982). The described core is probably from a breccia associated with the fault zone. The inferred detachment fault reflection is discontinuous across the Superstition Mountain Fault and is presumably truncated

C-2 STACK

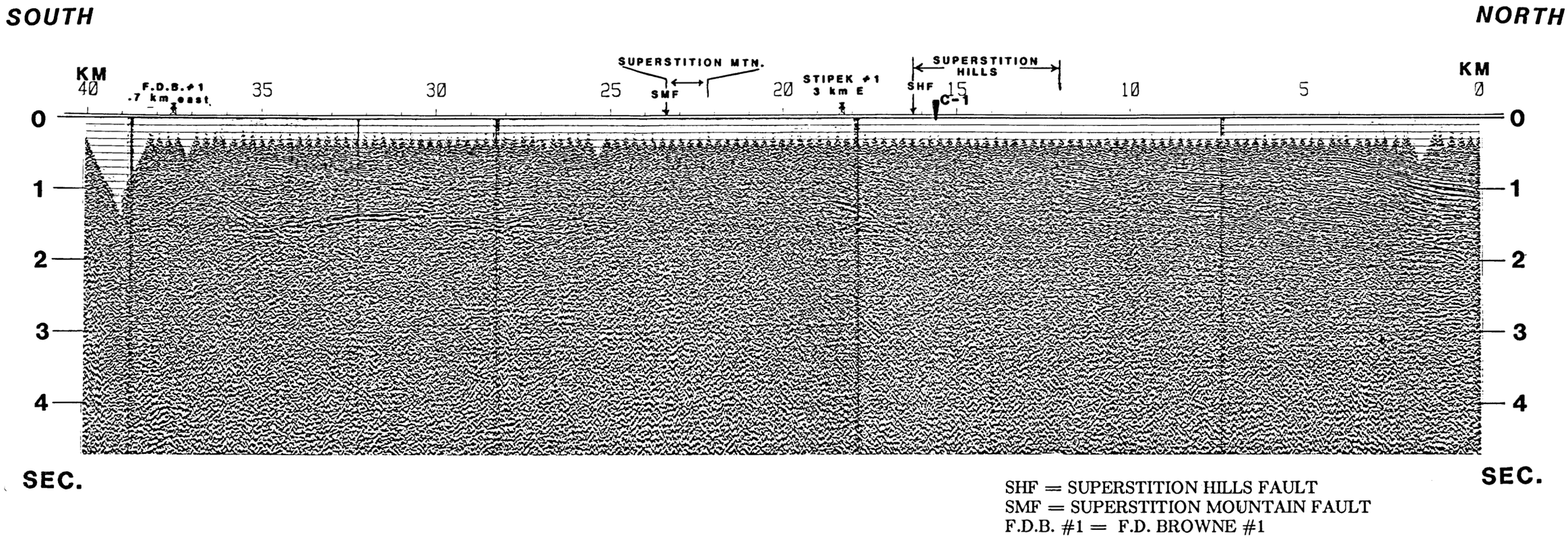

SHF = SUPERSTITION HILLS FAULT
SMF = SUPERSTITION MOUNTAIN FAULT
F.D.B. #1 = F.D. BROWNE #1

FIGURE 10. STACKED SECTION OF LINE C-2.

by the fault. Gravity measurements are not useful in this area for tracing the detachment fault, since the high associated with the granitic rocks of Superstition Mountain to the west of Line C-2 dominates the gravity data.

Detailed geological field work to identify and map detachment faults has not been done in the Coyote Mountains to the west of Line C-2 (Figure 5). However, Isaac *et al.* (1986) reported that Plio-Pleistocene detachment faults exist in the Yuha Desert region in northern Baja California. The faults are associated with hydrothermal mineralization and are inferred to be related to the opening of the Gulf of California. Therefore, the question arises as to whether the detachment fault identified in Line C-2 is mid-Tertiary in age and associated with the widespread detachment faulting which occurred throughout the southwestern United States (Frost and Martin, 1982; Frost *et al.*, 1982) or whether the fault is younger and related to the development of the Salton Trough.

The Superstition Hills (kilometers 12 to 16) and Superstition Mountain (kilometers 22 to 24) are characterized by zones with no reflectors (Figure 10). Their associated faults, the Superstition Hills and Superstition Mountain faults do not image. Since this line intersects these faults at angles of 40 and 30 degrees, respectively, the fault zone may have a dispersive effect on the incident wavefield. A possible diffraction associated with a high amplitude north-dipping reflector (Figure 10) is observed at kilometer 17 between the Superstition Hills and Superstition Mountain faults. This reflector is similar in amplitude and frequency (low) to the detachment fault reflection and is interpreted here as being the basement reflector. This interpretation is highly speculative since there is little well coverage in this region and, as mentioned previously, the gravity high associated with Superstition Mountain dominates the area and obscures more subtle trends. Texaco Stipek #1, total depth 2636 m, located 3 km east of Line C-2, encountered only clays, sands, and shales tentatively assigned to the Brawley, Borrego and Imperial Formations (Figure 4) (Dibblee, 1984). The diffraction observed in the dipping fault surface is probably due to faulting of the basement as it is compressed between the Superstition Hills and Superstition Mountain faults. If this reflector is

indeed from a detachment surface it would be highly significant since the block between the Superstition Hills and Superstition Mountain faults is inferred to have been translated 25 km from the southern section of the Brawley Seismic Zone (Fuis *et al.*, 1982).

Line C-2 shows a fairly simple structure for the sediments to the north of the Superstition Hills (kilometers 12 to 16). They dip gently to the north toward the Salton Sea which is expected since the Salton Sea formed at the topographically lowest portion of the Imperial Valley.

3.2.3 Line C-3

Line C-3, a 24-fold Vibroseis line shot in 1972, extends 11 km southwest from the Salton Sea (Figure 5). The profiles were 48-channel, split-spread, recorded with a sweep of 7 to 56 Hz. Group interval was 50.3 (165 ft). The field records were correlated with a shortened sweep to obtain 11.6 s of data. Automatic gain control (AGC) was applied to the uncorrelated shot gathers. In this process, termed Vibroseis whitening (Coruh and Costain, 1983), trace-scaling by AGC before sweep cross-correlation reduces the effect of high-amplitude components while enhancing low-amplitude ones, and, thus, compensates for frequency attenuation. The net result is that, after cross-correlation with the sweep, low-amplitude, high-frequency events are enhanced (Coruh and Costain, 1983). In the case of Line C-3, AGC before correlation (2 s operator) had the same effect as the application of a deconvolution operator. High frequencies were not appreciably enhanced. Figure 11 shows a portion of the stacked section with AGC before correlation and without. The section with AGC before correlation has a less "ringy" appearance but this is probably due to spike suppression and shallow reflectors are more coherent but lower frequency.

This line extends from the shore of the Salton Sea into the western San Felipe Hills (Figure 5). From northeast to southwest, the line passes over Quaternary alluvium, the sands and clays of the lacustrine Borrego Formation, and the sandstones and clays of the nonmarine Palm Spring Formation. Since the Palm Spring Formation

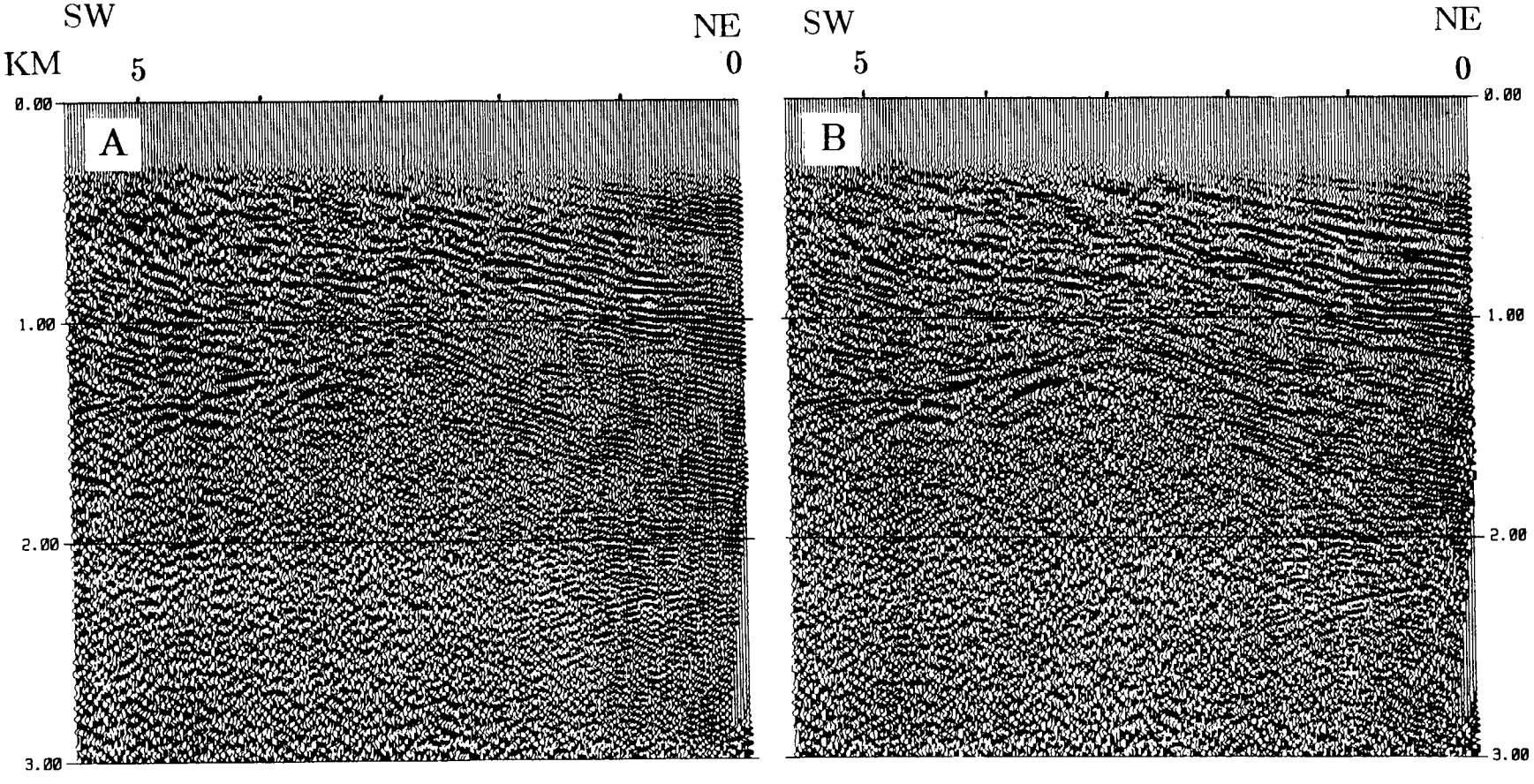

Figure 11. Portion of Line C-3 without (B) and with (A) AGC before correlation. Lower-frequency appearance of section B (with AGC) is probably due to spike-attenuation on un-correlated shot gathers rather than spectrum whitening.

grades upward into the Borrego Formation a major reflector is not expected at their contact. Only two wells were proximal to this line and logs were not available for either one. Pure Oil Co. Truckhaven #1, 4 km northwest of the line (kilometer 8), found biotite gneiss at 1784 m depth after drilling through the Palm Spring, Imperial and Split Mountain Formations (Dibblee, 1984). Tomahawk San Felipe #1, 7 km to the south (not shown on the section since it is so distant from the line), drilled 2135 m through sediments and was completed in the Split Mountain Formation (Calif. Div. of Oil and Gas, 1982).

Since logs were unavailable for these wells, the projection of the Brawley, Palm Spring and Imperial Formations into the seismic section was accomplished by extending the mapped contacts into the section using surface dips (Figure 5) (Dibblee, 1984). The Split Mountain Formation, since it was encountered at depth in wells to the north and south of the line, is assumed to lie below the Borrego, Palm Spring and Imperial Formations. In this region, the Split Mountain Formation unconformably overlies the Mesozoic basement. The Imperial Formation, which rests depositionally on the Split Mountain Formation, grades upwards into the Palm Spring Formation which, in turn, grades upwards into the Borrego Formation. Because of these relationships between rock units, a major reflection is expected only at the basement contact. This is what is observed in the seismic section (Figure 12).

The high-amplitude, northeast-dipping reflector at about 1.5 s is inferred to be the top of the gneissic basement. This interpretation is based on the identification of biotite gneiss from the Pure Oil Truckhaven #1 well. The basement reflector is broken by a major normal fault at kilometers 1 to 3 (Figures 12 and 13). The section of the basement which is downdropped to the northeast is not imaged. The faulted basement surface forms a gentle syncline which was formed prior to faulting. The sediments of the Palm Spring, Imperial, Borrego Formations to the south of the fault-block (kilometer 3) show onlap onto the basement surface. To the north the sediments appear uniform in thickness and do not exhibit growth features. This implies that sedimentation post-dates basement deformation and that normal-faulting is older than late Pliocene,

C-3 MIGRATION

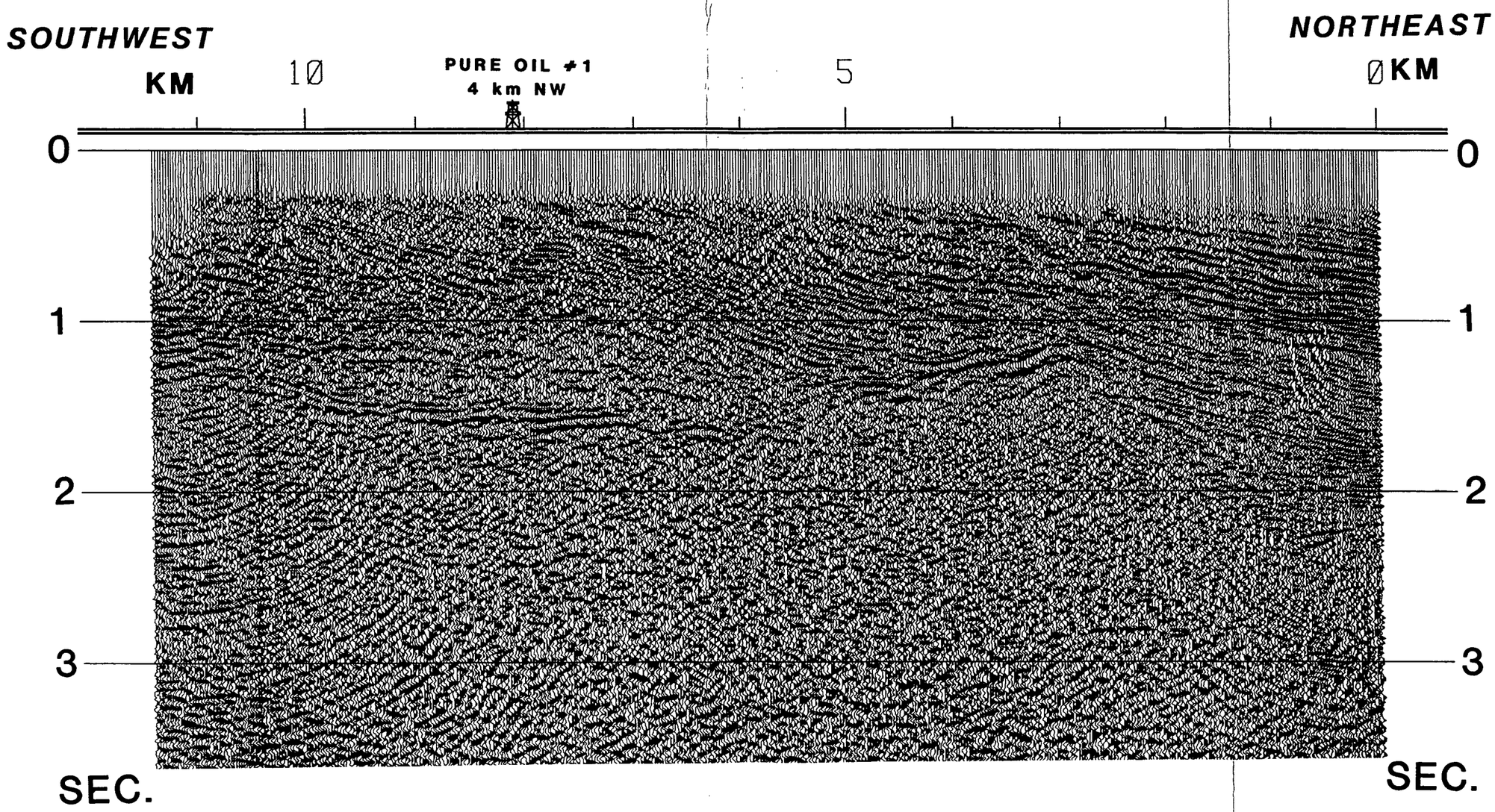

FIGURE 12. MIGRATED SECTION OF LINE C-3.

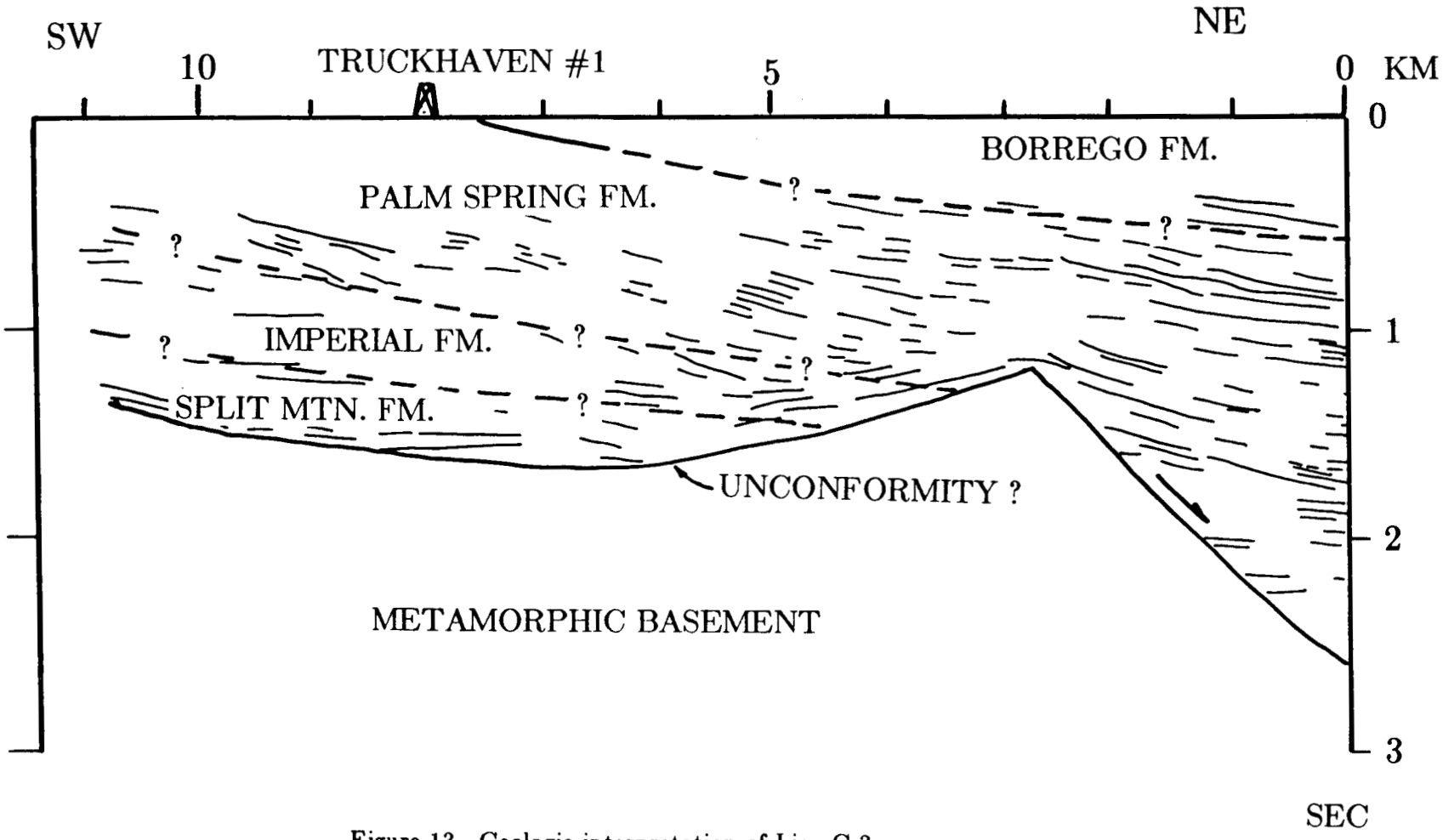

Figure 13. Geologic interpretation of Line C-3.

the age of the Palm Spring Formation (Winker, 1987), and, if the Imperial and Split Mountain Formations are present at depth, the age could be Miocene.

The geometry of the rock units in Figure 13 and the inferred age of the basement faulting suggest that the basement fault may have been involved in the formation of the Salton Trough. As the trough opened, the basement rocks were faulted and blocks were "calved" into the widening rift.

Prior to the re-processing of these data, it had been hoped that this line would image a detachment surface exposed at the surface, 17 km to the northwest, in the Santa Rosa Mountains (E.G. Frost, pers. comm. 1987). At that location upper plate, predominantly north-dipping, Tertiary sediments rest on a low-angle east-dipping detachment surface which formed at the contact with the mylonitic gneissic basement. Deep-seismic reflection profiles in the Whipple Mountains of California show that mylonitic fabric can image as well-layered reflections (Figure 16). Line C-3 does not exhibit a well-layered reflective fabric at depth. Thus, the basement reflector in Line C-3 is not interpreted as a fault but as an unconformity (Figure 4). This implies that the detachment fault (if it extends to this locale) is located within basement rocks. A reflection would not be expected from a fault imbedded within crystalline rocks unless the fault zone was wide enough, and altered enough, to generate an impedance contrast. A sketch of the possible relationship of the detachment fault to Line C-3, consistent with observed surface geology (Dibblee, 1984), is sketched in Figure 14. Note that in the line drawing (Figure 13) the Split Mountain Formation has been shown as conformable with the Imperial Formation while in the sketch it is unconformable. Either of these is possible because the Split Mountain Formation does not outcrop at this location and its presence is known only from wells.

Several studies by CALCRUST have been successful, using extended correlation of shallow seismic data, in imaging deep crustal reflectors and the Mohorovic Discontinuity (e.g. Galvan and Frost, 1985). The stack of Line C-3 extended to 11.6 s shows that there are no coherent reflectors visible below 2.5 s (Figure 15). There are many discrete events present but from an examination of the field gathers and from the

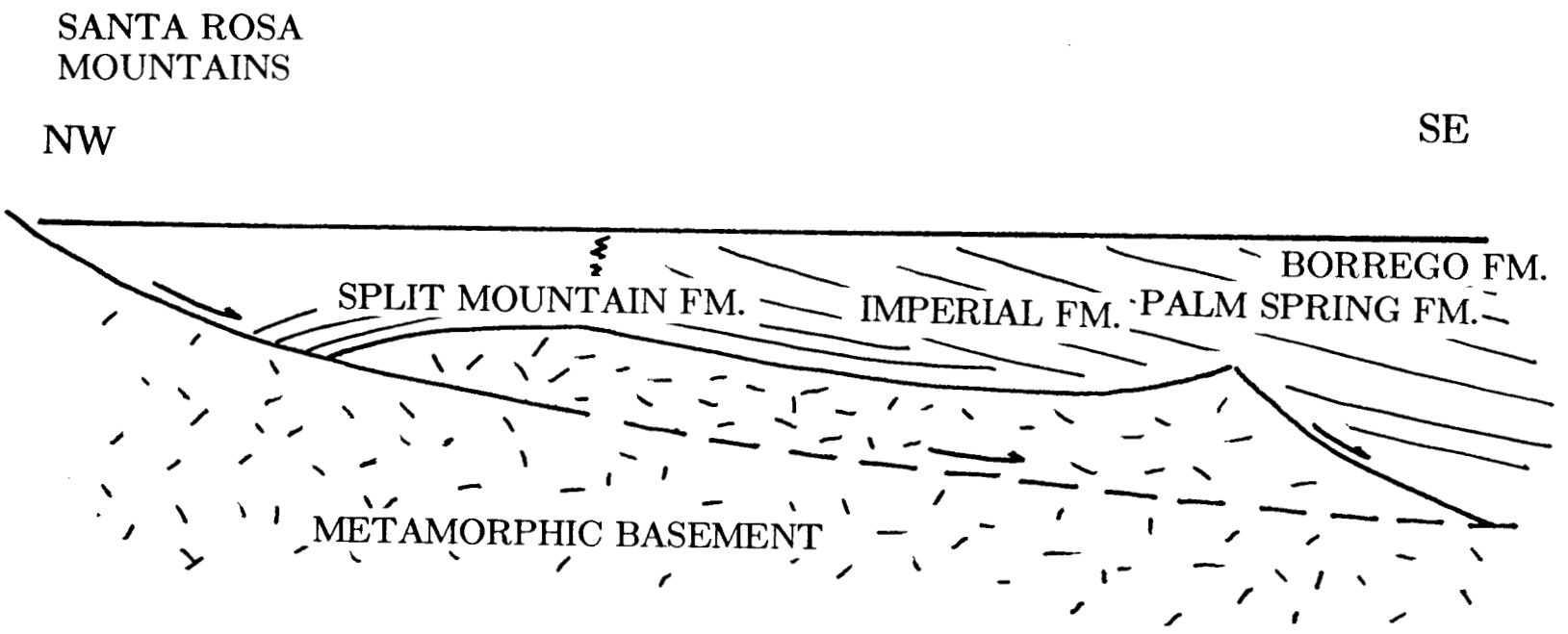

Figure 14. Speculative cross-section from Santa Rosa Mountains to Line C-3.

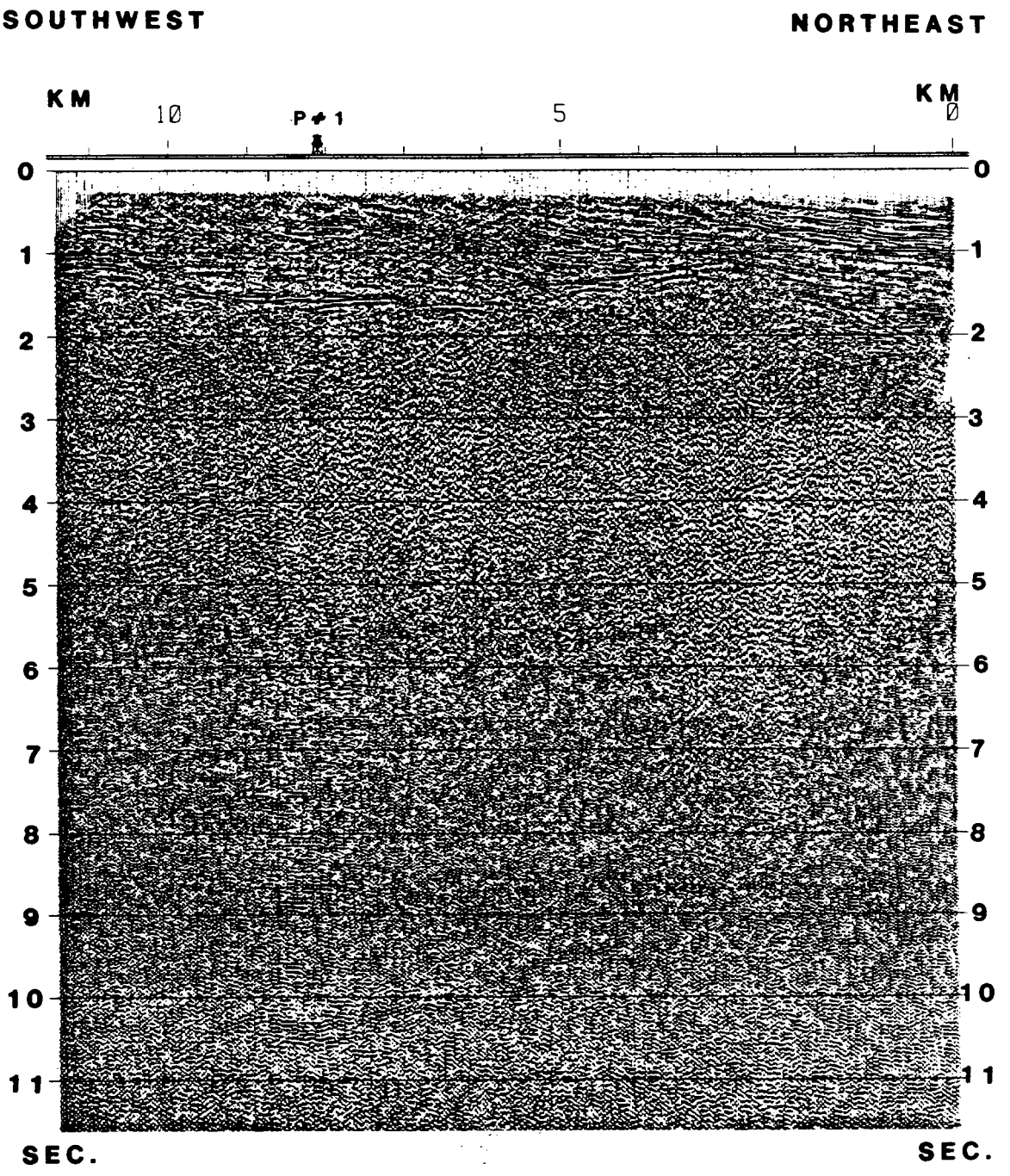

Figure 15. Stacked section of Line C-3. (P#1 = Pure Oil Truckhaven #1).

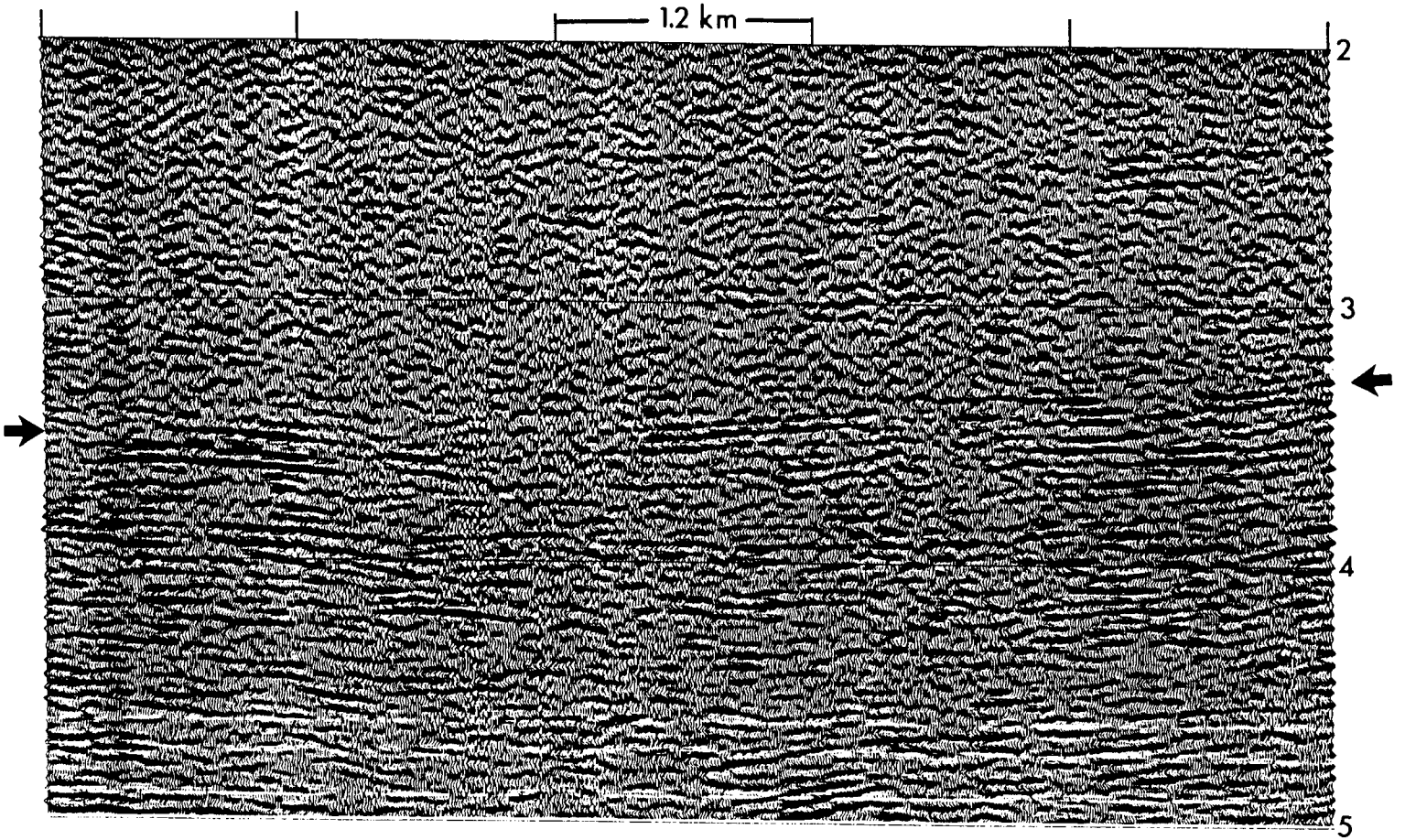

Figure 16. Portion of CALCRUST seismic profile from the Whipple Mountains, CA. The well-layered fabric below 3 s is interpreted as a mylonitic front. Directly from Frost and Okaya (1986).

velocity analysis it was decided that these events were not "real" seismic reflectors but were noise and artifacts of Vibroseis correlation. The lack of deep reflectors could be a result of the field parameters and geometry used. This line was shot in 1972 using four vibrators, 48-channel, split-spread profiles with 11 sweeps per profile and a group interval of 165 feet. The data were collected over a terrain of poorly consolidated sediments and alluvium. Under these field conditions it would be difficult to transmit seismic energy to deep crustal levels. Shot noise was present in nearly all of the field gathers (Figure 7). Re-shooting this line with a larger shot spread (i.e. more channels per shot) and smaller group intervals may be more successful in imaging the subsurface. The redundancy of the common depth point method is increased greatly with the large, multi-channel (e.g. 196, 256, and even 400-channel) systems that are available today. The longer spreads would also lessen the effect of shot noise since traces exhibiting this noise could be omitted and yet high subsurface coverage maintained.

The lack of deep reflectors in this region may also be due to complex geology that does not image clearly in a seismic reflection survey. The evolution of continental pull-apart basins is not well understood but the process of breaking continental crust and infilling the rift with mantle material must involve the fracturing and melting of the country rock. A pull-apart basin does not suddenly come into existence but involves the destruction of older pull-aparts by younger ones as rifting evolves (Mann *et al.*, 1983). Thus, the edge of the Pacific Plate, as it exists in this region, has probably been modified by melting and extension so that velocity and density contrasts have been softened.

3.3 Eastern Imperial Valley

The locations of the seismic lines in the eastern Imperial Valley provide an opportunity to verify the existence of the Sand Hills Fault, Algodones Fault and/or faulting related to the East Highline Canal seismicity lineament (Figure 6). Each of these faults has been proposed as the southerly extension of the San Andreas Fault by various authors (Babcock, 1971; Crowell and Ramirez, 1979; Heath, 1980) based mostly on

surficial evidence consisting of lineaments mapped from aerial photographs. Figure 6 shows these faults and the seismicity lineament as mapped by Fuis *et al.* (1982) from seismicity and seismic refraction data. They associated the Algodones and Sand Hills faults with changes in the slope of the basement.

All of the seismic lines in this side of the Imperial Valley, except Line E-3 and E-4, are proximal to known geothermal areas (Palmer *et al.* , 1975). This affords the chance to further study the seismic expression of geothermal reservoirs that was first discussed in Section 3.3.1 with respect to Line C-1.

3.3.1 Line E-1

Line E-1 extends for 85 km from just north of Niland, California southeast to the U.S.-Mexican border (Figure 6). Tapes of the stacked section were provided by Exxon so that migration was possible. This Vibroseis-source line was recorded in 1973 with 48-channel, split-spread shots spaced at 100.6 m (330 ft) intervals. The geophone interval was also 100.6 m (330ft). An 11 s sweep of 8 to 36 Hz was used and 30 sweeps were stacked at each shot point. The same recording geometry and parameters were used for all of the Exxon lines in this study. Four seconds of data in Line E-1 were migrated using a constant velocity of 2 km/s which was determined from tests using different constant migration velocities. Line E-1 follows the proposed trace of the Sand Hill Fault.

The migrated section shows that shallow reflectors rest on an undulating, faulted surface which lies at 1 to 2 s across the section (Figure 17). From cross-lines E-2, E-3, and E-5 it can be seen that this surface dips to the southwest. Ajax U.S.L. Phyllis #1 (kilometer 45), drilled in 1955 to a total depth of 1 km, reached metamorphic rock at .9 km (Figure 6) (Kovach *et al.* , 1962). Using a constant velocity of 2.1 km/s (Kovach *et al.* , 1962) a two-way travel time of .9 s is calculated. Allowing that the well is a distance of 12 km from the line and basement dips to the west, it is reasonable to interpret this basement reflector as the top of upper-plate granitic rocks of the Chocolate Mountain Thrust system (Figure 6).

E-1 MIGRATION

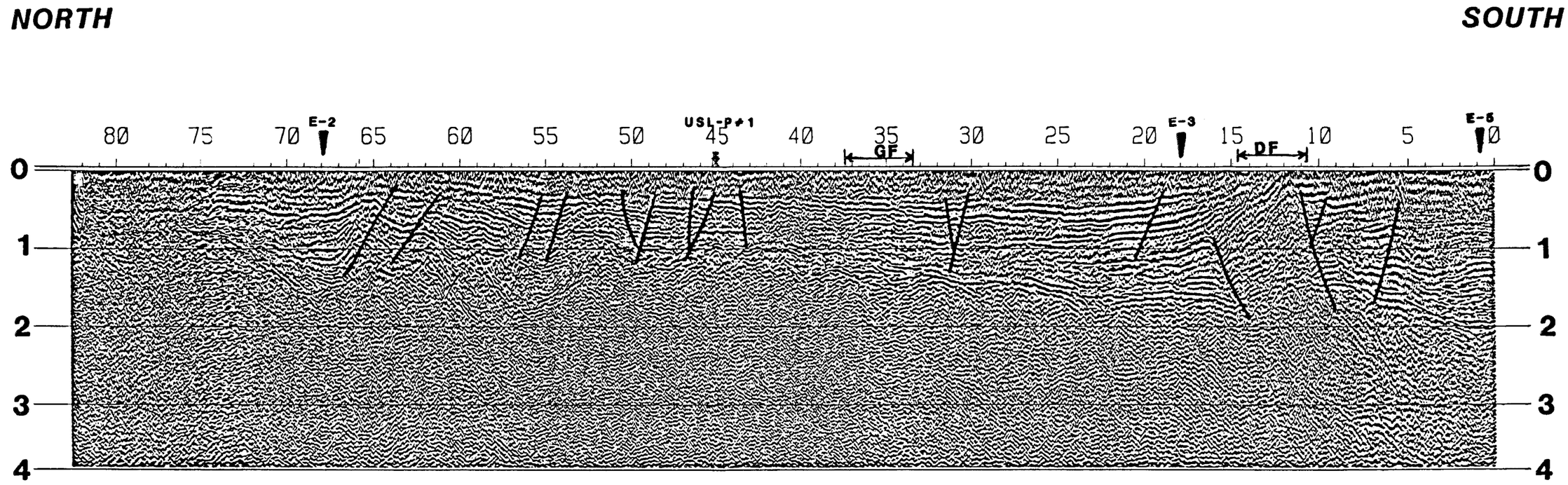

FIGURE 17. MIGRATED SECTION OF LINE E-1.

The numerous faults which are imaged in Line E-1 display reverse (e.g. kilometer 65), strike-slip (e.g.kilometer 10), and normal (e.g. kilometer 20) motion. This is consistent with the model developed by Sylvester and Smith (1976) for the geometrical relations of faults within a transpressional environment. Their strain ellipse diagram showed that parallel to a major strike-slip fault it is possible to encounter all three types of faults which are seen in Line E-1. This line is oriented roughly along the strike of the Salton Trough (Figure 2).

Different generations of folding and faulting appear to have occurred. At kilometer 11, faulting has penetrated to the surface while, at kilometer 16, sediments appear to onlap the tilted block at 1 s implying that the fault at kilometer 11 is younger than the fault at kilometer 16. Faulting of the basement, in general, does not seem to penetrate the surface sediments.

Line E-1 passes to the east of the Dunes (kilometer 11 to 15) and West Glamis (kilometer 34 to 37) geothermal fields (Figure 6). Both of these geothermal fields are associated with anomalous near-surface temperature gradients of up to 20° C/100 m (Palmer *et al.*, 1975). The association of the Dunes geothermal field with deformed and faulted sediments is obvious (Figure 17). The seismic expression of the Glamis temperature gradient anomaly is more subtle. The sediments are not deformed but they show the same "fading" that is seen in the Brawley, East Brawley, and Dunes geothermal fields. The lack of deformation of the shallow sediments at the Glamis geothermal field shows that major faulting is not necessary for the migration of hot brines to the near surface. The fact that the basement is shallow near Glamis is probably the reason for the development of a temperature gradient anomaly in this area. Bouguer gravity maxima, associated with densification of sediments by hydrothermal alteration, occur at the Dunes and Glamis geothermal fields (Elders, 1979). Since stacking velocities were not available for this line it could not be determined if high seismic velocities were associated with the anomalies as they are at Brawley and East Brawley.

3.3.2 Line E-2

Line E-2 is an east-west profile that begins at the foot of the Chocolate Mountains, crosses the East Highline Canal seismicity lineament, and terminates in the Salton Sea geothermal field (Figure 6). AGC with a 1.5 s operator was used before correlation (see section 3.2.3). Many of the shots were "ringy" so a 30 ms deconvolution operator was applied. Extended correlation was used to increase the field record length to 13 s.

There are a few fragmented reflections below 3 s but, as in Line C-3, coherent energy is absent at depth (Figure 18). Two lines not processed for this study, but shot by Exxon using the same recording parameters and geometry, are located near the Cargo Muchacho Mountains (Figure 6). These lines were named E-6 and E-7 for reference. They were re-correlated to 12 s and show coherent reflectors at depth (Figures 19 and 20) Re-recording the reflection profile, changing the spread-length or group interval as well as varying other field parameters, might be more effective at imaging deep crustal structure. The poor imaging at depth of the Imperial Valley lines argues that this region may be a "bad data" area where it is difficult to transmit seismic energy to great depths. This may be due to subsurface geology that is complex causing ray path distortion or perhaps the high heat and partial melt of continental rifting lessens impedance contrasts. Shot amplitudes from Lines E-3 and E-6 (Figure 6) will be compared in Section 3.3.3 for further analysis of this topic.

In Line E-2 sediments display a gradual thickening to the west (Figure 21). This sedimentary wedge is broken by numerous strike-slip faults which exhibit good flower structure. In this profile, there is no high amplitude reflection(s) associated with the top of the granitic basement. Rather the top of basement is inferred by a change in reflectance and from Line E-1. Line E-2 crosses the East Highline Canal seismicity lineament, as shown by Fuis *et al.* (1982), at about kilometer 7. The character of the seismic section at this location is slightly different than surrounding fault blocks in that sediments dip more steeply to the west and are lower in amplitude. The change in slope across the lineament may indicate strike-slip displacement. In Line C-1 (Plate 1),

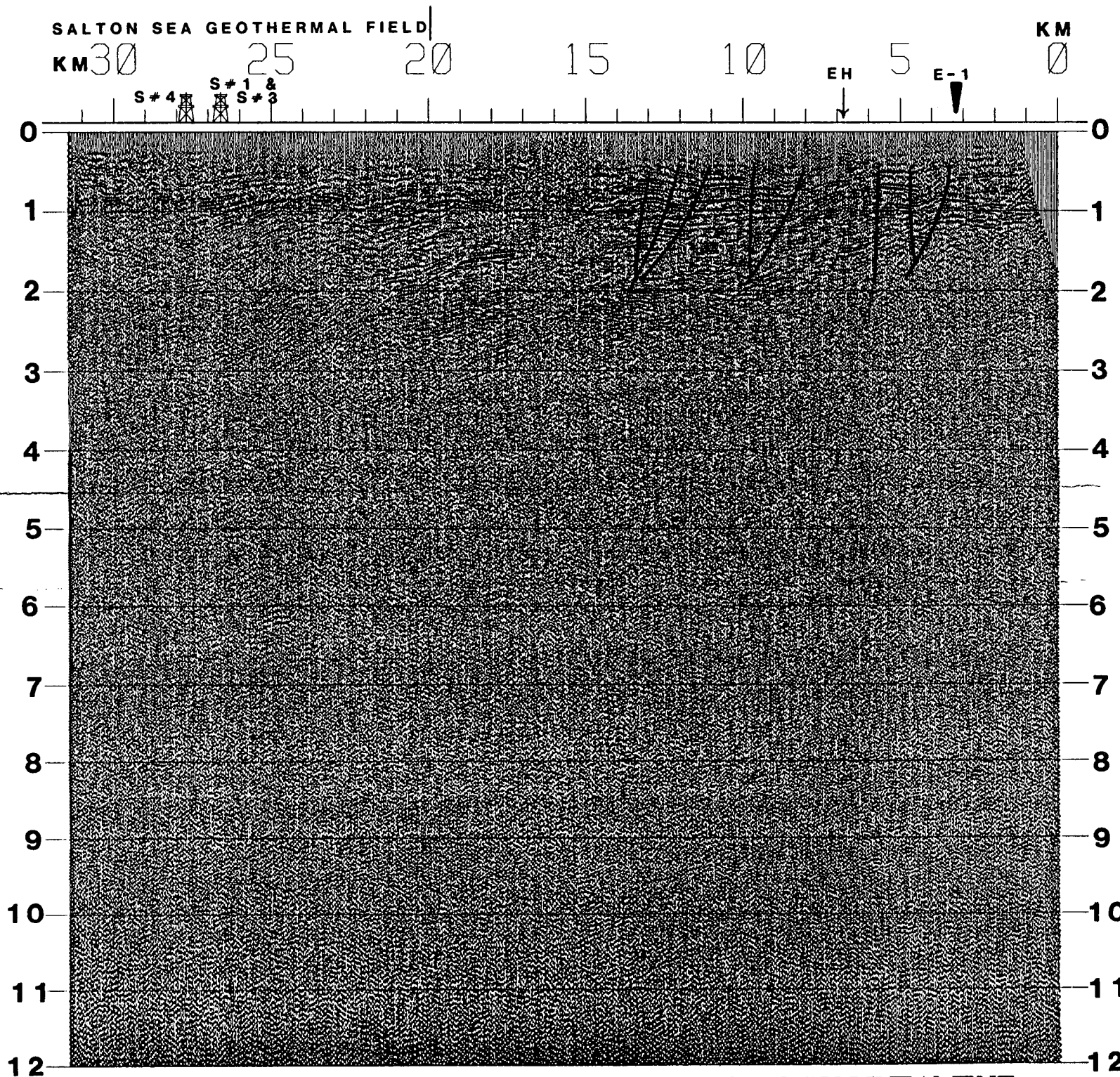

FIGURE 18. STACKED SECTION OF LINE E-2.

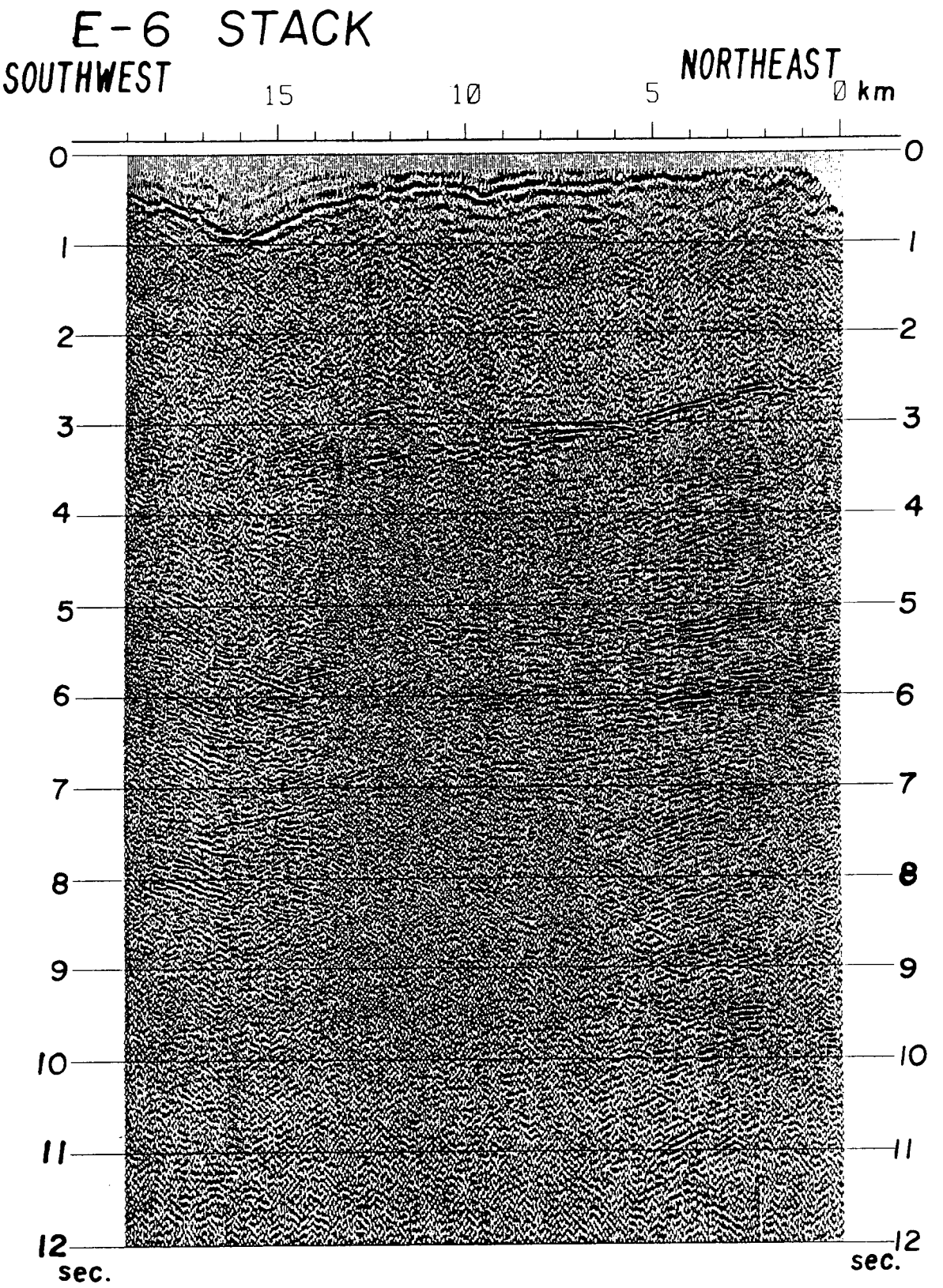

Figure 19. Stacked section (Line E-6) from the Cargo Muchacho Mountains.

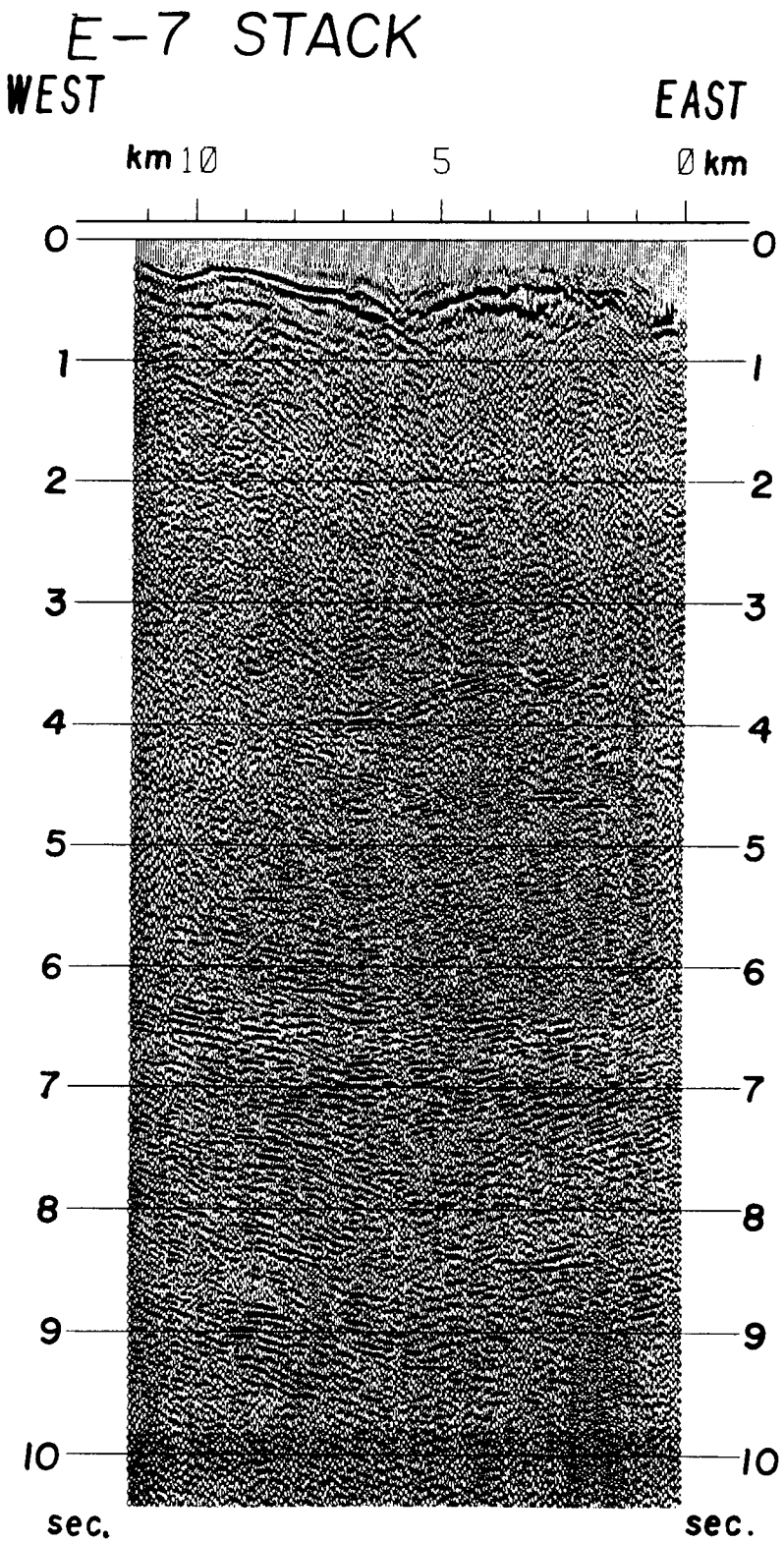

Figure 20. Stacked section (Line E-7) from the Cargo Muchacho Mountains.

E-2 MIGRATION

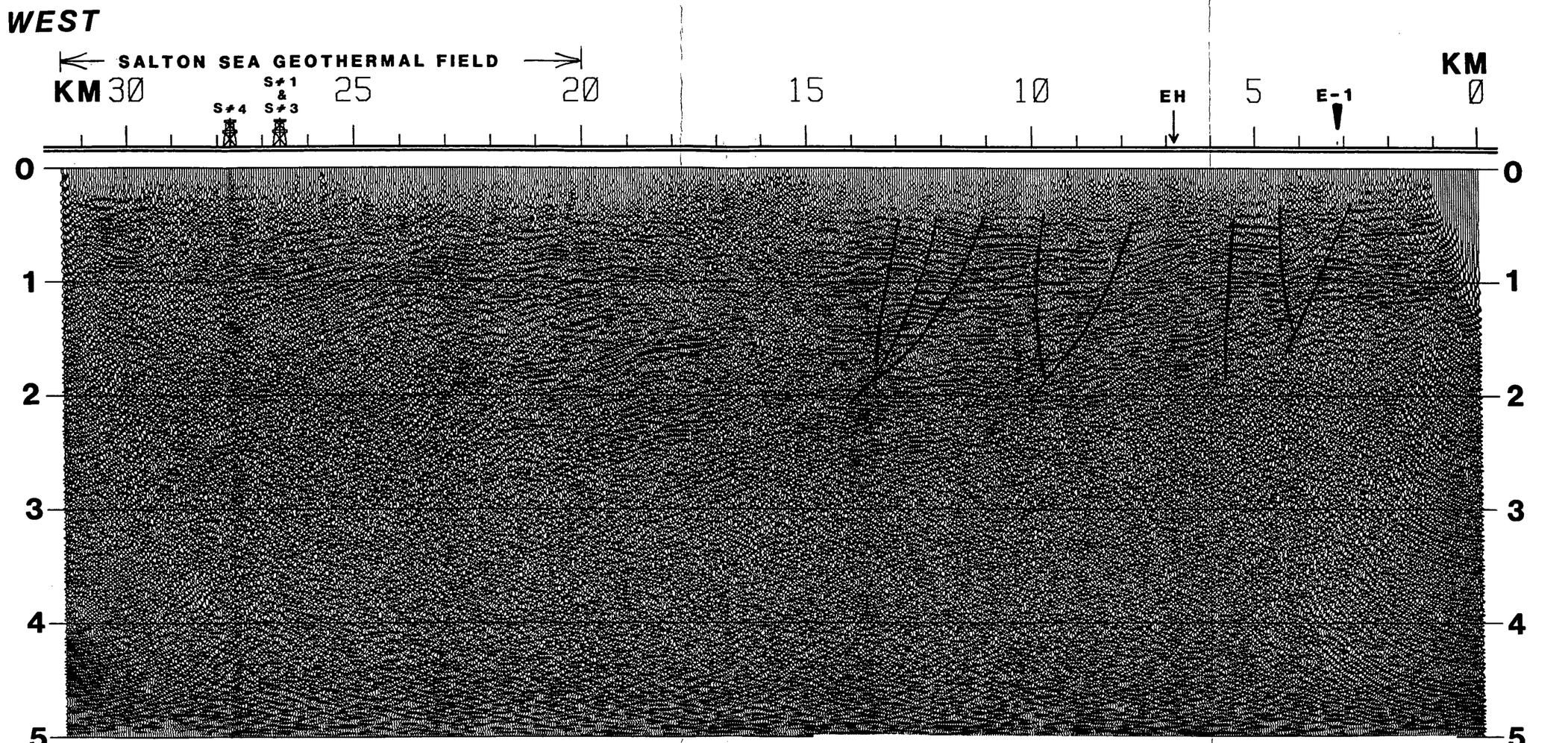

FIGURE 21. MIGRATED SECTION OF LINE E-2.

the East Highline Canal seismicity lineament was associated with a similar change in slope. This implies that a 16 km long, strike-slip fault may join Lines C-1 and E-2. It would be interesting to examine the seismic expression of the San Andreas Fault, where it has been mapped on the ground surface just to the northwest of these lines (Figure 2), and compare the results with what has been observed in this study.

This line terminates in the southern portion of the Salton Sea geothermal field (kilometer 20 to 32). As in the Brawley and East Brawley geothermal fields, there is a loss in seismic resolution in the geothermal area. This geothermal field is associated with a Bouguer gravity high and is one of the two geothermal fields (the other is Cerro Prieto) in the Imperial Valley which have surface expression in recent volcanism, mud pots and hot springs (Elders, 1979; Muffler and White, 1969). Stacking velocities increase slightly to the west beneath the geothermal field instead of decreasing as would be expected because of the westward- thickening wedge of sediments.

Intense metamorphism is occuring in the sediments of the Salton Sea geothermal field. Deep wells indicate that greenschist-facies metamorphism is occurring at depths of 1 to 2.5 km (McDowell and Elders, 1979; Muffler and White, 1969). Younker *et al.* (1982) characterized the geothermal field based on geological, geophysical and thermal measurements and observations. They determined that the field has a variable thickness cap rock, 250 to 700 m, that consists of evaporites overlain by clay, sand, silt and gravel. They divided the reservoir into slightly altered upper reservoir rocks extensively altered lower reservoir rocks. In three wells, Sinclair Nos. 1, 3, and 4 (all at about kilometer 27) (Figure 21), the depth to the cap rock was estimated at about 300 m and the depth to the highly altered rocks of the lower reservoir was about 1000 m. Using a velocity model derived from a seismic refraction study by Frith (1978) (Figure 22), two-way travel times of .3 s and 1.1 s are calculated for the cap rock and the highly-altered sediments, respectively. In the seismic section, the top of the highly-altered rocks coincides with a loss in seismic resolution which is consistent with the loss of seismic resolution associated with the Brawley, East Brawley, Glamis, and Dunes geothermal fields.

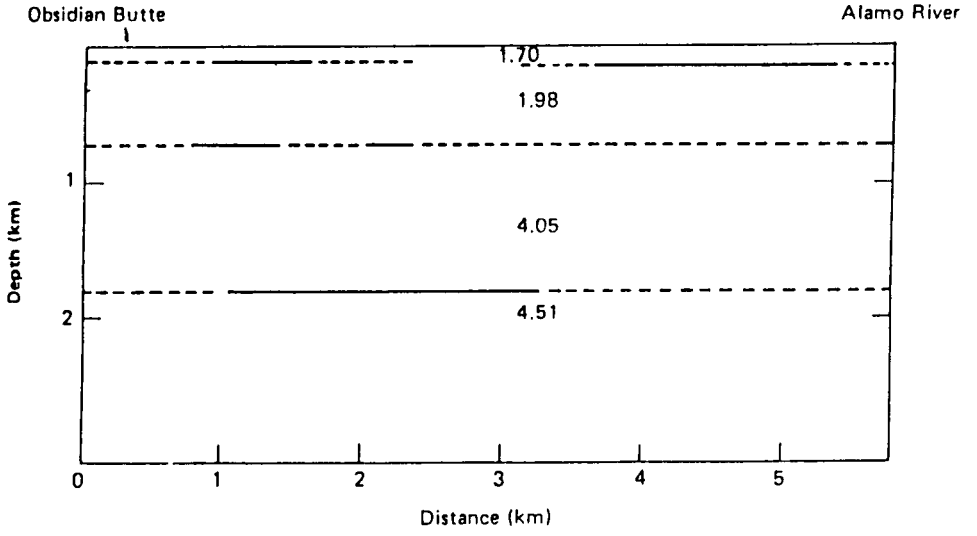

Figure 22. Velocity model for the Salton Sea geothermal field interpreted from seismic refraction profiles. Modified from Frith (1978). Velocities are in km/s.

3.3.3 Line E-3

Line E-3 runs from the Sand Hills southwest across East Mesa (Figure 6). It terminates at the edge of the East Mesa geothermal field. Traces were lengthened to 13 s by extended correlation. Tests showed that little improvement could be made in data resolution by applying AGC before correlation, so it was not used.

In this 16 km line, sediments, thickening to the west, are underlain by a steeply dipping reflector which is interpreted as the top of the crystalline basement (Figure 23). In the southern Chocolate Mountains, Proterozoic and Mesozoic metamorphic rocks have been thrust to the east over the Orocopia Schist. This complex is commonly referred to as the Chocolate Mountains thrust system. The basement reflection is from the top of the upper plate metamorphic rocks. Line E-6, 12 km to the east of Line E-3 (Figure 6), has a set of high amplitude, west-dipping reflections at about 3 s which are interpreted as the base of the Orocopia Schist (Figure 19) (Morris *et al.*, 1986). If these reflections are projected to Line E-3 they should appear at the eastern edge of the section at about 5 s. Thus, a faint, west-dipping reflective sequence at about 5.5 s at kilometer 0 is interpreted as the base of the Orocopia Schist (Figure 24). Above that is another faint sequence which starts at 3.5 s. These reflections have been tentatively identified as the top and the base of the lower plate Orocopia Schist (Figure 24). These reflectors plus the basement reflector disappear at about kilometer 8.

Sedimentary reflectors above the basement are discontinuous across the seismic section and, to the west, from kilometers 9 through 16, they are folded into an anticline and syncline pair (Figure 23). This line crosses the Sand Hills Fault, as shown by Fuis *et al.* (1982), at about kilometer 1. This fault is proposed by some workers to be the extinct extension of the San Andreas Fault (Babcock, 1971). A fault has been interpreted in the sediments near this location. However, it does not penetrate the basement as would be expected of the San Andreas fault. The Sand Hills/San Andreas fault is more likely located at about kilometer 6 where there is a change in the reflective character of the sediments, indicating the possible juxtaposition of blocks of differing stratigraphy by strike-slip movement. This fault would also truncate the

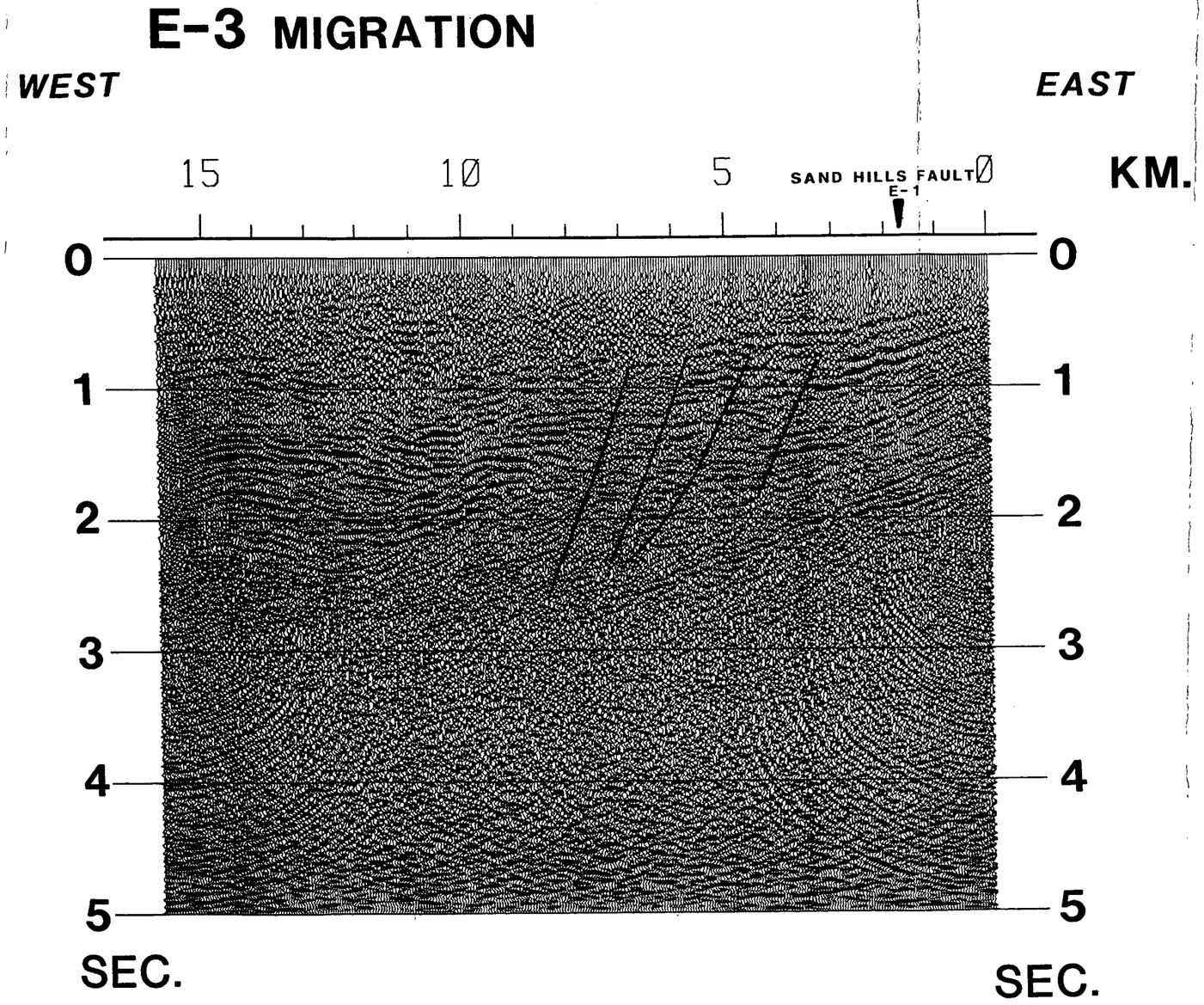

FIGURE 23. MIGRATED SECTION OF LINE E-3.

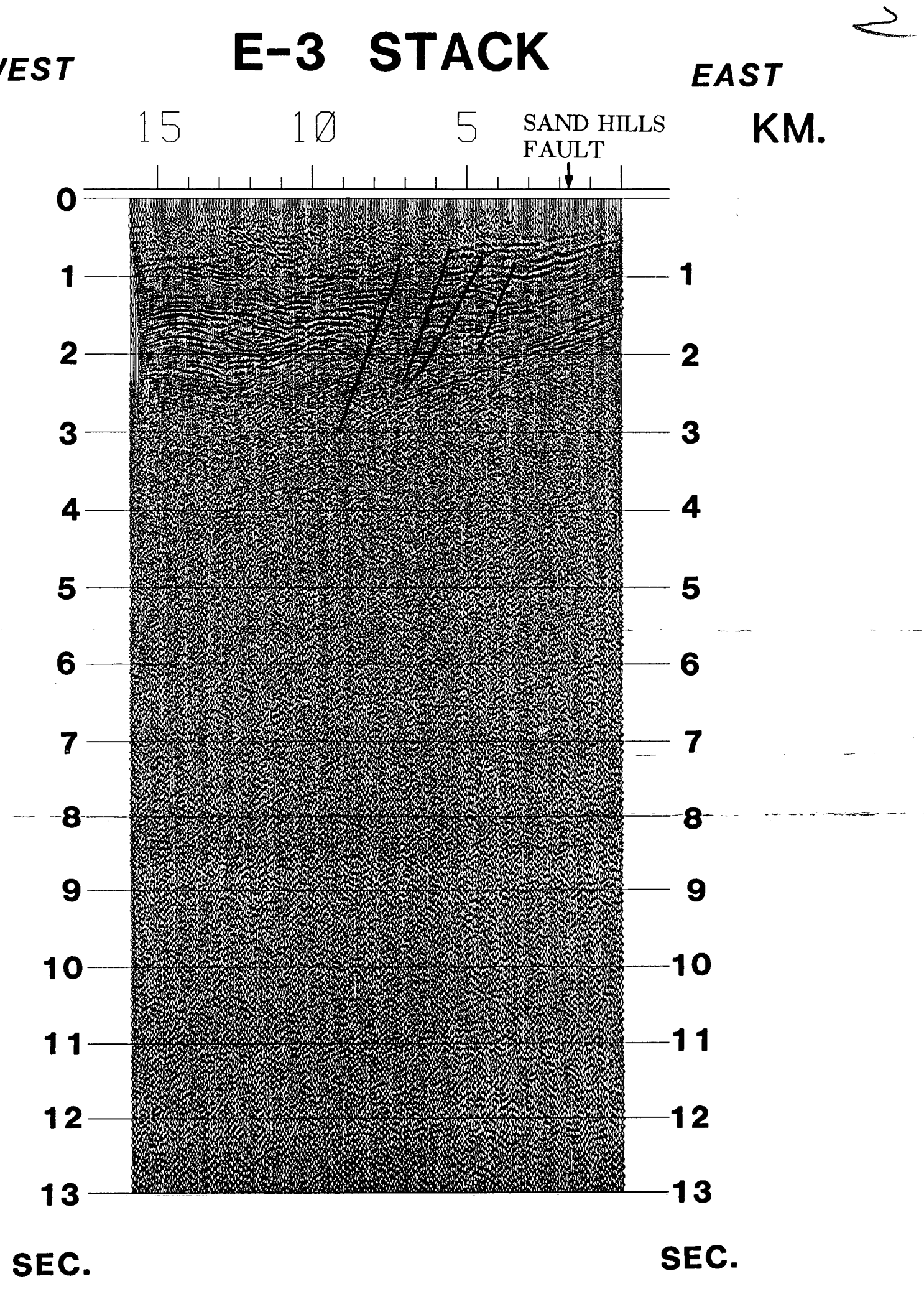

FIGURE 24. STACKED SECTION OF LINE E-3.

crystalline rocks of the Chocolate Mountains thrust system.

As in Lines C-3 and E-2, there are no distinctive seismic reflectors or patterns at deep levels in Line E-3 (other than those from the Chocolate Mountains thrust system) (Figure 24). Shot amplitudes from channel 12 of three shots from each line were plotted (Figure 25). These traces have been correlated only, no gain has been applied. Zero dB corresponds to the maximum amplitude of a trace. The traces from Line E-6, a line with deep reflectors, all show the expected amplitude decay (1/r) from energy loss due to spherical divergence. On the other hand, the traces from Line E-3 show very little amplitude decay with time. This indicates a high "noise" level and any reflections occuring at depth might be imperceptible from the background noise. This test does not preclude the fact that deep reflectors may not exist at depth within the Imperial Valley, However, it does show that changes in shot and/or recording parameters for these lines (E-1 through E-5) that lessen the effect of the noise could make possible the recording of deep data from within the Imperial Valley.

3.3.4 Lines E-4 and E-5

Lines E-4 and E-5 overlap each other for about 2 km but they are offset by about 305 m (Figure 6). Together they extend for 40 km west from the Sand Hills, past the Border geothermal area, and into the Imperial Valley.

The subsurface imaging in Line E-5 is very poor (Figure 26). There are only two strong, coherent reflectors in the section. An undulating, west-dipping reflector, at 1.3 to 2.3 s, is interpreted as the basement reflector (Figure 26). Basement, mafic orthogneisses and granites, outcrops about 6 km to the east in the Cargo Muchacho Mountains. Line E-1, which intersects this line at kilometer 8.5, shows no unusual occurrence that would explain the high amplitude of the other strong reflector in Line E-5. It appears, in Line E-1, as part of a fairly flat-lying sequence of sedimentary rocks. In this line, both the basement and overlying reflector are folded.

As in Lines E-2 and E-3 the Sand Hills Fault coincides with a fault in the seismic data which adjoins two blocks of differing seismic character and breaks the basement

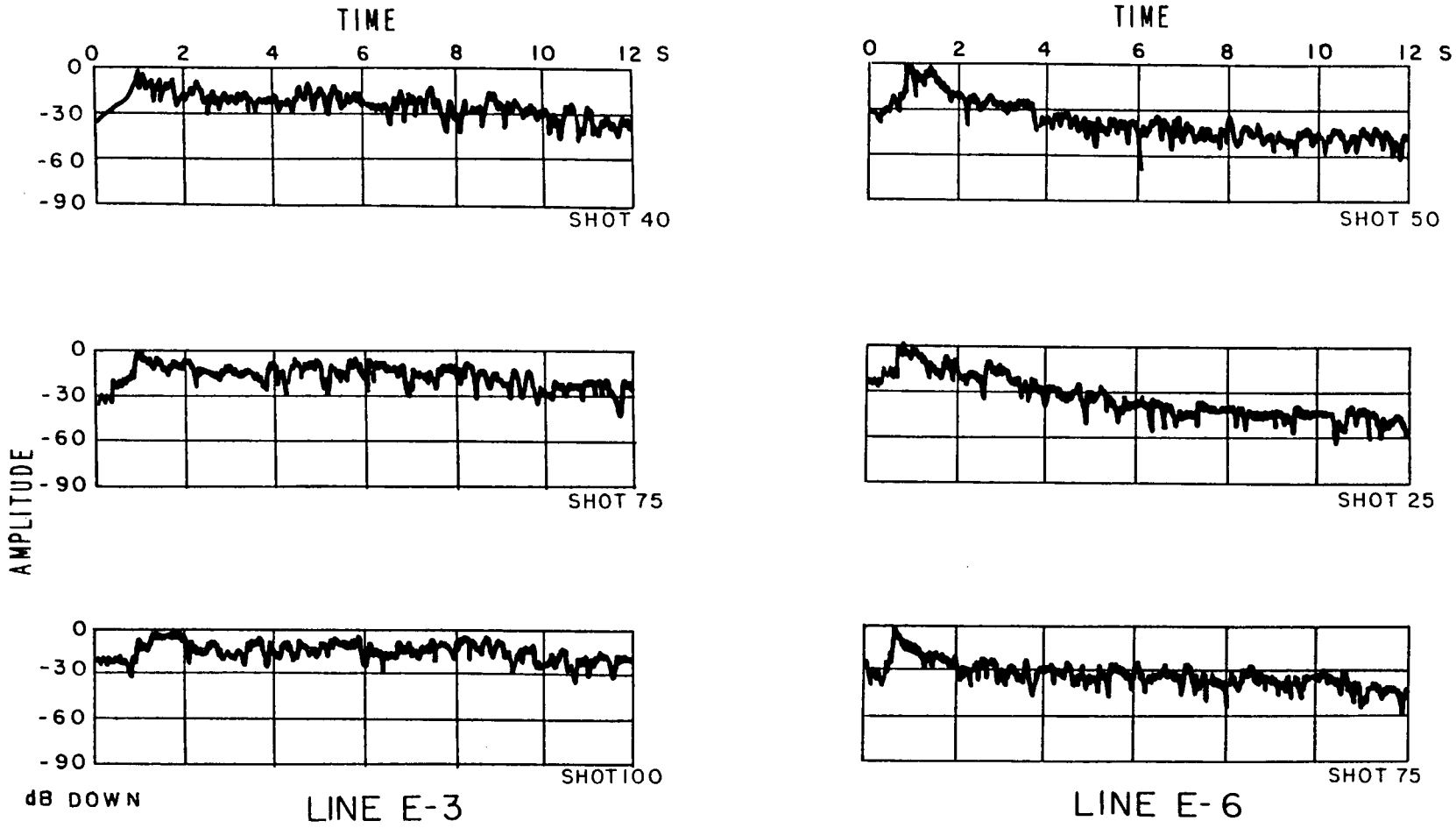

Figure 25. Comparison of shot amplitudes between Line E-3 and Line E-6. Traces are scaled so that the highest amplitude corresponds to 0 dB. All traces shown are from channel 12.

E-5 MIGRATION

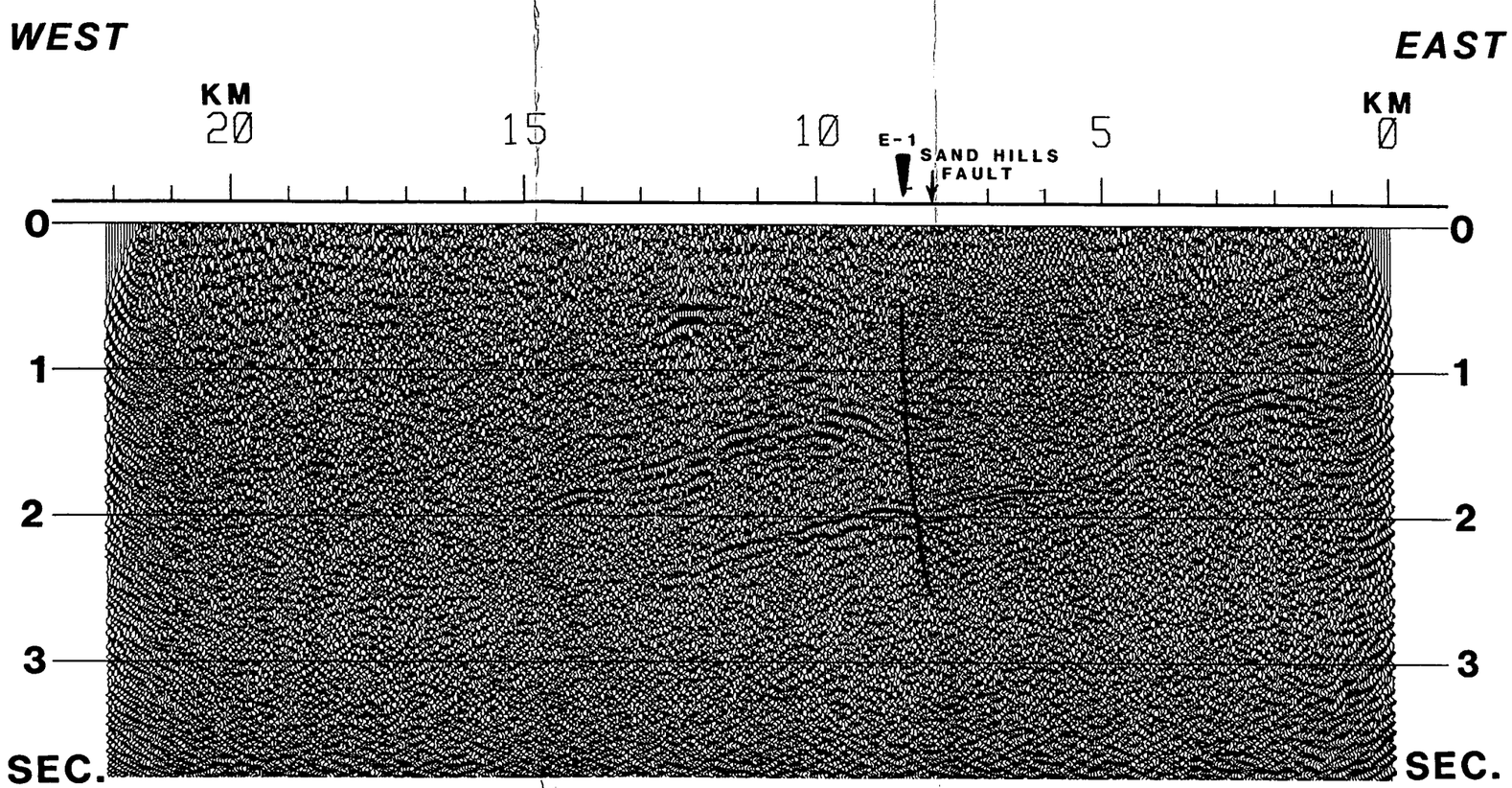

FIGURE 26. MIGRATED SECTION OF LINE E-5.

reflector. The evidence from these three lines leads to the conclusion that the Sand Hills Fault is indeed the southerly extension of the San Andreas Fault.

This observation lends support to the proposition that the Rand and Pelona Schists, located several hundred kilometers to the northeast of the Imperial Valley, are the same unit as the Orocopia Schist in the Chocolate Mountains, but have been translated part of the way to their current locations by the Sand Hills (i.e. San Andreas Fault) (Haxel and Dillon, 1978) Also, this implies that the western boundary of the crystalline rocks of the Chocolate Mountains thrust system (i.e. the pre-rift North American plate boundary) extend at least as far west as this location.

Upon concluding that the Sand Hills Fault is the southern extension of the San Andreas Fault the next step is whether or not it can be linked to the East Highline seismicity lineament. At this time there is no convincing evidence to support a decision in either direction but trenching and the study of aerial photographs by Heath (1980), which delineated several small northwest-trending faults in the region between Lines E-10 and E-3, suggests that the two may be connected.

The sediments shown in Line E-4 are deformed by several faults (Figure 27). These faults correspond to the location where Line E-4 passes through the southern portion of the Border geothermal anomaly, at kilometers 4 through 7. The sediments in this area have been tilted and growth structure can be seen at kilometers 7 through 8. The basement reflector is not seen in this section as sediments thicken to the west.

3.4 Synthesis

The eight seismic reflection profiles in this study display features which are consistent with the idealized map of a pull-apart basin proposed by Crowell (1974) (Figure 28). The Salton Trough is a northwest-trending topographic and structural depression which marks the boundary between the Pacific and North American plates in southeastern California. The Imperial Valley is located where the plate boundary changes from a series of right-stepping spreading centers to the transcurrent tectonics of the San Andreas fault system. The northernmost of the series of *en echelon*

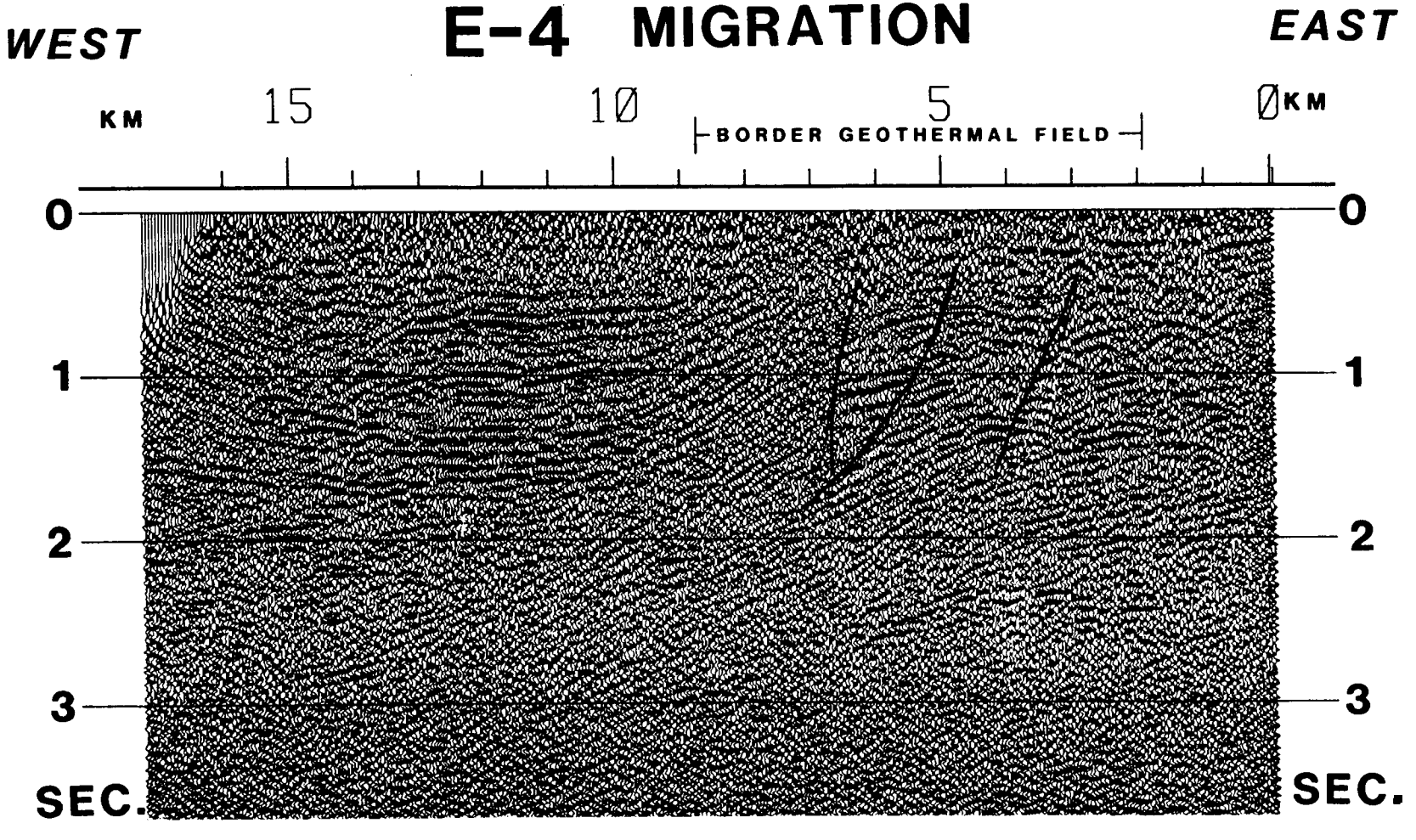

FIGURE 27. MIGRATED SECTION OF LINE E-4.

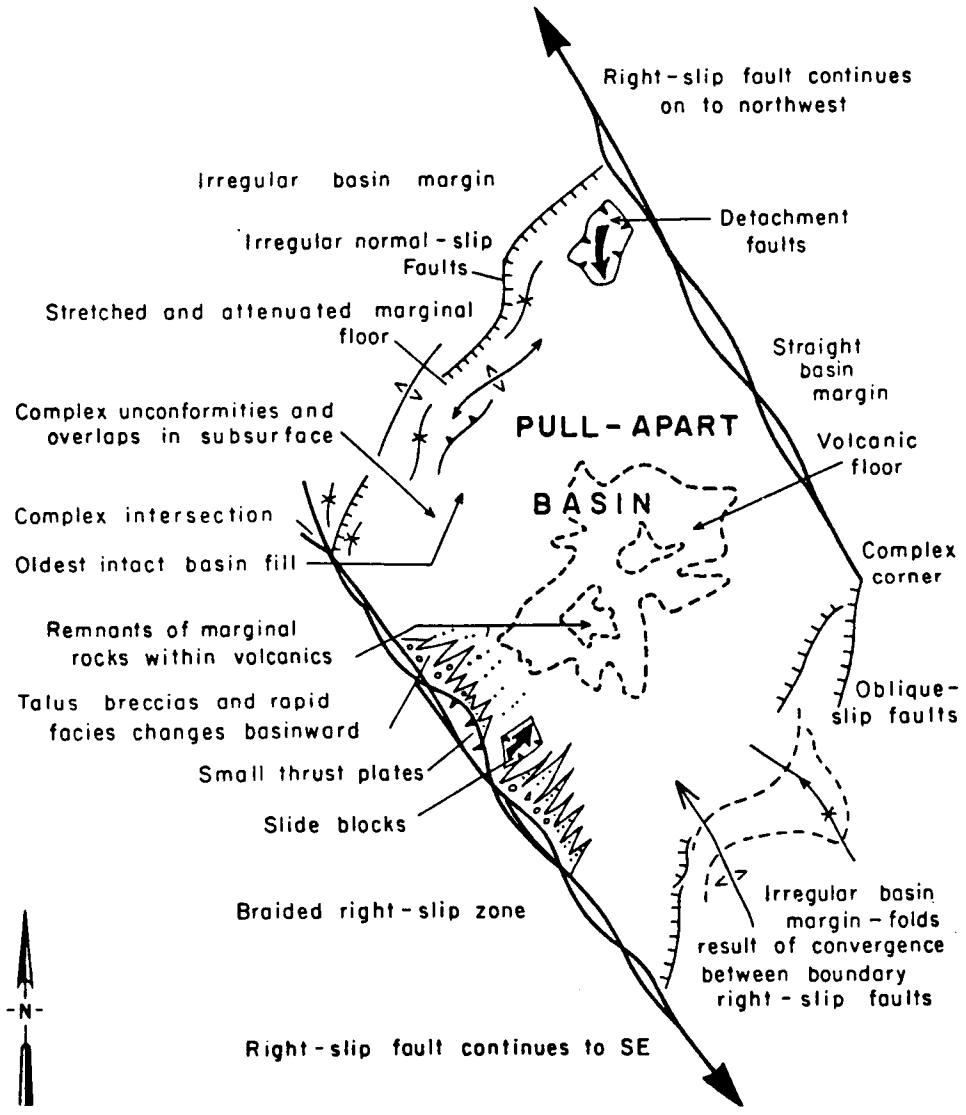

Figure 28. Sketch map of features of idealized pull-apart basin. Directly from Crowell (1974).

spreading centers is inferred to occur in the Imperial Valley beneath deep sediments at the Brawley Seismic Zone.

Figure 28 illustrates many of the structural features which are found in an idealized pull-apart basin. Several of these features were imaged by the seismic reflection profiles in this study. For example, the northwest-trending major faults in the sketch would be analogous to the San Andreas (north) and Imperial (south) faults. The thickening of sediments towards the center of the basin was evident in several of the seismic lines. Slide blocks and detachment faults were imaged in Lines C-2 and C-3 and both reverse and normal faulting were shown in Line E-1.

All of the seismic lines exhibited pervasive, mostly strike-slip faulting of the surface sediments. The slight growth structure shown in some of the fault blocks indicates that slip between the San Andreas and Imperial faults is accomodated near the surface by sporadic movement on these faults. The near-surface layer of sediments can be envisioned as a mosaic of blocks which are 'jostled' together as movement occurs on the San Andreas and Imperial faults.

CHAPTER 4
CONCLUSIONS

The youthful and active nature of the transtensional Imperial Valley is well displayed in these seismic reflection profiles. The detailed picture of the central basin reveals a wedge of sediments that thins to the east. This wedge is broken by numerous faults, most of which are strike-slip in agreement with the regional stress pattern (Figure 1). There is evidence for block rotations, on the scale of 5 to 10 kilometers, occurring within the region where strike-slip motion is transferred from the Imperial to the San Andreas fault.

These lines provide insight into the nature of the east and west edges of the Imperial Valley. The basement at the northwestern margin of the valley, to the north of the Superstition Hills, has been normal-faulted and blocks of basement material have "calved" into the the trough. A blanket of sediments has been deposited on this margin. In the Superstition Hills and Superstition Mountains area, rocks that are presumably the oldest in the basin have been "squeezed" up at the restraining bend of the Superstition Hills fault and within the transpressional environment of the Superstition Mountain Fault. To the south of these hills, the top of the basement is a detachment surface that dips gently into the basin. This margin is also covered by a thick sequence of sediments. The basement of the eastern margin consists of metamorphic rocks of the upper plate of the Chocolate Mountain Thrust system underlain by the Orocopia Schist. These rocks dip to the southeast and extend westward to the Sand Hills Fault but do not appear to cross it. Thus, the Sand Hills Fault is interpreted to be the southern extension of the San Andreas Fault. North of the Sand Hills Fault the East Highline Canal seismicity lineament is associated with a strike-slip fault and is probably linked to the Sand Hills Fault.

Although a good picture of the shallow crustal structure of the Imperial Valley was obtained, the use of the extended correlation failed to image deep structure. The meta-sedimentary basement is non-reflective and structures deeper than about 4 s are not seen. This, of course, means that the Mohorovic Discontuity was not imaged. The

lack of deep reflections may be due to inappropriate recording parameters and geometry or the lack of reflectors may be real. Relative amplitude tests indicate that reflections may be "buried" within the high level of ambient noise present in the data or attenuated in saturated, heterogenous sediments.

In addition to heat flow and Bouguer gravity anomalies this study confirmed the findings of Blakeslee (1984) and van de Kamp *et al.* (1978), that geothermal reservoirs are related to zones of poor or faded reflectivity and high seismic velocities. Six geothermal areas crossed by these lines, Salton Sea, Dunes, Glamis, Brawley, East Brawley and Border, were associated with "faded" zones, Bouguer gravity maxima and, when data were available, with higher velocities than the surrounding terrane. The combination of all these characteristics make a useful tool in the delineation of geothermal reservoirs.

References

Adams, M.A., F.L. Hillemeyer, and E.G. Frost, Anastomosing shear zones - a geometric explanation for mid-Tertiary crustal extension in the detachment terrane of the Colorado River region, California, Arizona, and Nevada, *Geol. Soc. Am. Abstr. Programs, 15,* 375, 1983.

Allen, C.R., M. Wyss, J.N. Brune, A. Grantz, and R.E. Wallace, Displacements on the Imperial, Superstition Hills, and San Andreas faults triggered by the Borrego Mountain earthquake, *U.S. Geol. Surv. Prof. Pap., 787,* 87-104, 1972.

Atwater, T., Implications of plate tectonics for the Cenozoic evolution of North America, *Geol. Soc. Amer. Bull., 81,* 315-349, 1970.

Babcock, E.A., Detection of active faulting using oblique infrared aerial photography in the Imperial Valley, California, *Geol. Soc. Am. Bull., 82,* pp. 3189-3196, 1971.

Biehler, S., Geophysical study of the Salton Trough of southern California, Ph.D. dissertation, 139 pp., Calif. Inst. of Technol., Pasadena, 1964.

Biehler, S., R.L. Kovach, and C.R. Allen, Geophysical framework of northern end of Gulf of California structural province, *Mem. Am. Assoc. Pet. Geol. 3,* 126-143, 1964.

Blakeslee, S., Seismic discrimination of a geothermal field: Cerro Prieto, *Geothermal Res. Counc. Trans., 8,* 183-188, 1984.

Brook, C.A., and C.W. Mase, The hydrothermal system at the East Brawley KGRA, Imperial Valley, California, *Geothermal Res. Counc. Trans., 5,* 157-160, 1981.

California Division of Oil and Gas, Well summary report, Texaco F. D. Browne #1, Sec. 6, T. 16S, R. 12E, Imperial Co., Calif., 10 pp., 1952.

California Division of Oil and Gas, Well summary report, Tomahawk San Felipe #1, Sec. 29, T. 11S, R. 10E, Imperial Co., Calif., 1982.

Champion, D.E., D.G. Howell, and C.S. Gromme, Paleomagnetic and geologic data indicating 2500 km of northward displacement for the Salinian and related terranes, California, *J. Geophys. Res., 89,* 7736-7752, 1984.

Coney, P.J., Mesozoic-Cenozoic cordilleran plate tectonics, *Mem. Geol. Soc. Am. 152,*

33-50, 1978.

Coruh, C, and J.K. Costain, Noise attenuation by Vibroseis whitening (VSW) processing, *Geophys., 48,* 543-554, 1983.

Cox, A., Rotation of microplates in western North America, *Geol. Assoc. Can. Spec. Pap., 20,* 305-321, 1980.

Crowell, J.C., Origin of Late Cenozoic basins in southern California, in *Soc. Econ. Paleon. Mineral. Spec. Pub., 22,* 190-203, 1974.

Crowell, J.C., An outline of the tectonic history of south-eastern California, in *The Geotectonic Development of California, Rubey Volume 1,* edited by W.G. Ernst, pp. 583-600, Prentice-Hall, Englewood Cliffs, N.J., 1981.

Crowell, J.C., and V.R. Ramirez, Late Cenozoic faults in southeastern California, in *Tectonics of the Juncture Between the San Andreas Fault System and the Salton Trough, Southeastern California,* edited by J.C. Crowell and A.G. Sylvester, pp. 27-39, Department of Geological Sciences, University of California, Santa Barbara, Calif., 1979.

Dibblee, T.W. Jr., Geology of the Imperial Valley region, California, *Calif. Div. Mines Bull., 170,* 21-28, 1954.

Dibblee, T.W. Jr., Stratigraphy and tectonics of the San Felipe Hills, Borrego Badlands, Superstition Hills, and vicinity, in *The Imperial Basin-Tectonics, Sedimentation, and Thermal Aspects,* edited by C.A. Rigsby, pp. 31-44, Soc. Econ. Paleontol. and Mineral., Pacific Section, Sacramento, California, 1984.

Dillon, J.T., Geology of the Chocolate and Cargo Muchacho Mountains, southeasternmost California, Ph.D. Dissertation, 405 pp., Univ. of Calif., Santa Barbara, 1975.

DiPippo, R., Geothermal power plants, worldwide status - 1986, *Geothermal Res. Counc. Bull., 15,* 9-18, 1986.

D'Onfro, P. and P. Glagola, Wrench fault, southeast Asia, in *Seismic Expression of Structural Styles,* edited by A.W. Bally, pp. 4.2-9 - 4.2-12, Studies in Geology Series 15, American Association of Petroleum Geologists, Tulsa, Oklahoma, 1983.

Doser, D.I., and H. Kanamori, Spatial and temporal variations in seismicity in the Imperial Valley (1902-1984), *Bull. Seismol. Soc. Am., 76,* 421-438, 1986.

Ehlig, P.L., Origin and tectonic history of the basement terrane of the San Gabriel Mountains, central Transverse Ranges, in *The Geotectonic Development of California, Rubey Volume 1,* edited by W.G. Ernst, pp. 253-284, Prentice-Hall, Englewood Cliffs, N.J., 1981.

Elders, W.A., The geological background of the geothermal fields of the Salton Trough, in *Guidebook: Geology and Geothermics of the Salton Trough,* edited by W.A. Elders, pp. 1-19, Geological Society of America, Boulder, Colo., 1979.

Elders, W.A., R.W. Rex, T. Meidav, P.T. Robinson, and S. Biehler, Crustal spreading in southern California, *Science, 178,* 15-24, 1972. Elders, W.A., and L.H. Cohen, *The Salton Sea geothermal field, California as a near-field natural analog of a radioactive waste repository in salt,* 138 pp, BMI/ONWI-513, Office of Nuclear Waste Isolation report, 1983.

Engel, A.E.J., and P.A. Schultejahn, Late Mesozoic and Cenozoic tectonic history of south central California, *Tectonics, 3,* 659-675, 1984.

Frith, R.B., A seismic refraction investigation of the Salton Sea geothermal area, Imperial Valley, California, M.S. thesis, University of California, Riverside, 1978.

Frost, E.G. and D.A. Okaya, Application of seismic reflection profiles to tectonic analysis in mineral exploration, *Frontiers in Geology and Ore Deposits of Arizona and the Southwest,* edited by B. Beatty and P.A.K. Wilkinson, pp. 137-151, Arizona Geological Society Digest Volume XVI, Tucson, Arizona, 1986.

Frost, E.G., and D.L. Martin (Eds.), *Mesozoic-Cenozoic Tectonic Evolution of the Colorado River Region, California, Arizona, and Nevada, Anderson-Hamilton Volume,* 608 pp., Geological Society of America, Boulder, Colo., 1982.

Frost, E.G., T.E. Cameron, and D.L. Martin, Comparison of Mesozoic tectonics with mid-Tertiary detachment faulting in the Colorado River area, California, Arizona, and Nevada, in *Geologic Excursions in the California Desert,* compiled by J.D. Cooper, pp. 113-159, Geological Society of America, Cordilleran Section, 1982.

Frost, E.G., D.L. Martin, and D. Krummenacher, Mid-Tertiary detachment faulting in southwestern Arizona and southeastern California and its overprint on the Vincent thrust system, *Geol. Soc. Am. Abstr. Programs, 14,* 164, 1982.

Frost, E.G., and D.L. Martin, Overprint of Tertiary detachment deformation on the Mesozoic Orocopia Schist and Chocolate Mountains thrust, *Geol. Soc. Am. Abstr. Programs, 15,* 577, 1983.

Fuis, G.S., Displacement on the Superstition Hills Fault triggered by the earthquake, *U.S. Geol. Surv. Prof. Pap., 1254,* 145-154, 1982.

Fuis, G.S., and M.R. Schnapp, The November-December 1976 earthquake swarms in the northern Imperial Valley, California: Seismicity on the Brawley fault and related structures, *EOS Trans. AGU, 58,* 1188, 1977.

Fuis, G.S., W.D. Mooney, J.H. Healy, G.A. McMechan, and W.J. Lutter, Crustal structure of the Imperial Valley region, *U.S. Geol. Surv. Prof. Pap., 1254,* 25-49, 1982.

Fuis, G.S., and W.M. Kohler, Crustal structure and tectonics of the Imperial Valley region, California, in *The Imperial Basin-Tectonics, Sedimentation, and Thermal Aspects,* edited by C.A. Rigsby, pp. 1-13, Soc. Econ. Paleontol. and Mineral., Pacific Section, 1984.

Fuis, G.S., W.D. Mooney, J.H. Healy, G.A. McMechan, and W.J. Lutter, A seismic refraction survey of the Imperial Valley region, California, *J. Geophys. Res., 89,* 1165-1189, 1984.

Galvan, G.S., and E.G. Frost, Seismic reflection evaluation of detachment-related deformation in the Transition Zone, west-central Arizona, *EOS Trans. AGU, 66,* 978, 1985.

Gibson, L.M., L.L. Malinconico, T. Downs, and N.M. Johnson, Structural implications of gravity data from the Vallecito-Fish Creek Basin, western Imperial Valley, California, in *The Imperial Basin-Tectonics, Sedimentation, and Thermal Aspects,* edited by C.A. Rigsby, pp. 15-30, Soc. Econ. Paleontol. and Mineral., Pacific Section, Sacramento, California, 1984.

Haxel, G.B., and J.T. Dillon, The Pelona-Orocopia Schist and Vincent-Chocolate Mountain thrust system, southern California, in *Mesozoic Paleogeography of the Western United States,* edited by D.G. Howell and K.A. Douglas, pp. 453-470, Soc. Econ. Paleontol. and Mineral., Pacific Section, Sacramento, California, 1978.

Haxel, G.B., and M.J. Grubensky, Tectonic significance of localization of middle Tertiary detachment faults along Mesozoic and early Tertiary thrust faults, southern Arizona region, *Geol. Soc. Am. Abstr. Programs, 16,* 533, 1984.

Haxel, G.B., R.M. Tosdal, and J.T. Dillon, Tectonic setting and lithology of the Winterhaven Formation: A new Mesozoic stratigraphic unit in southeasternmost California and southwestern Arizona, *U.S. Geol. Surv. Bull., 1599,* 19 pp., 1985.

Haxel, G.B., R.M. Tosdal, and J.T. Dillon, Field guide to the Chocolate Mountains Thrust and Orocopia Shcist, Gavilan Wash area, southeasternmost California, in *Frontiers in Geology and Ore Deposits of Arizona and the Southwest,* edited by B. Beatty and P.A.K. Wilkinson, pp. 282-293, Arizona Geological Society Digest Volume XVI, Tucson, Arizona, 1986.

Heath, E.G., Evidence of faulting along a projection of the San Andreas fault, south of the Salton Sea, in *Geology and Mineral Wealth of the California Desert,* edited by D.L. Fife and A.R. Brown, pp.467-474, South Coast Geological Society, Santa Ana, Calif., 1980.

Hill, D.P., P. Mowinckel, and L.G. Peake, Earthquakes, active faults, and geothermal areas in the Imperial Valley, California, *Science, 188,* 1306-1308, 1975.

Howell, D.G., J.K. Crouch, H.G. Greene, D.S. McCulloch, and J.G. Vedder, Basin development along the Late Mesozoic and Cainozoic California margin: A plate tectonic model of subduction, oblique subduction, and transform tectonics, *Spec. Pub. Int. Assoc. Sed., 4,* 43-62, 1980.

Howell, D.G., Tectonics of continent-ocean transect C-3, offshore southern California to central, New Mexico, *Geol. Soc. Am. Abstr. Programs, 16,* 545, 1984.

Isaac, S., T.K. Rockwell, and G. Gastil, Plio-Pleistocene detachment faulting, Yuha Desert region, western Salton Trough, northern Baja California, *Geol. Soc. Am. Abstr. Programs, 18,* 120, 1986.

Johnson, C.E., Cedar-An approach to the computer automation of short-period local networks; II, Seismotectonics of the Imperial Valley of southern California, Ph.D. dissertation, 332 pp., Calif. Inst. of Technol., Pasadena, 1979.

Johnson, C.E., and D.M. Hadley, Tectonic implications of the Brawley earthquake swarm, Imperial Valley, California, January 1975, *Bull. Seismol. Soc. Am., 66,* 1133-1144, 1976.

Johnson, C.E., and D.P. Hill, Seismicity of the Imperial Valley, *U.S. Geol. Surv. Prof. Pap., 1254,* 15-24, 1982.

Johnson, N.M., C.B. Officer, N.D. Opdyke, G.D. Woodard, P.K. Zeitler, and E.H. Lindsay, Rates of late Cenozoic tectonism in the Vallecito-Fish Creek basin, western Imperial Valley, California, *Geology, 11,* 664-667, 1983.

Keskinen, M., and J. Sternfeld, Hydrothermal alteration and tectonic setting of intrusive rocks from East Brawley, Imperial Valley: An application of petrology

to geothermal reservoir analysis, in *Proc. Eighth Workshop Geoth. Reservoir Eng.,* pp. 39-43, Stanford University, Stanford, California, 1982.

Kovach, R.L., C.R. Allen, and F. Press, Geophysical investigations in the Colorado delta region, *J. Geophys. Res., 67,* 2845-2871, 1962.

Lachenbruch, A.H., J.H. Sass, and S.P. Galanis, Jr., Heat flow in southernmost California and the origin of the Salton Trough, *J. Geophys. Res., 90,* 6709-6736, 1985.

Larson, R.L., H.W. Menard, and S.M. Smith, Gulf of California: A result of ocean-floor spreading and transform faulting, *Science, 161,* 781-784, 1968.

Lomnitz, C., C.R. Mooser, C.R. Allen, J.N. Brune, and W. Thatcher, Seismicity and tectonics of the northern Gulf of California region, Mexico-preliminary results, *Geofis. Int., 10,* 37-48, 1970.

Luyendyk, B.P., M.J. Kamerling, R.R. Terres, and J.S. Hornafius, Simple shear of southern California during Neogene time suggested by paleomagnetic declinations, *J. Geophys. Res.* 12,455-12,466, 1985.

McDowell, M., Overprint of Tertiary detachment faulting on the Winterhaven Formation in the Gavilan Hills, southeastern California, M.S. thesis, San Diego State University, San Diego, 1986.

McDowell, S.D., and W.A. Elders, Geothermal metamorphism of sandstone in the Salton Sea geothermal system, in *Guidebook: Geology and Geothermics of the Salton Trough,* edited by W.A. Elders, pp. 70-76, Geological Society of America, Boulder, Colo., 1979.

Mann, P., M.R. Hempton, D.C. Bradley, and K. Burke, Development of pull-apart basins, *J. Geol., 91,* 529-554, 1983.

Morris, R.S., E.G. Frost, and D.A. Okaya, Preliminary seismic reflection interpretation of the overprint of Tertiary detachment faulting on the Orocopia Schist-Chocolate Mountains Thrust system, Milpitas Wash area of southeastern California, in, *Cenozoic Stratigraphy, Structure, and Mineralization in the Mojave Desert,* pp. 123-126, Geological Society of America, Cordilleran Section, 1986.

Muffler, L.J.P., and D.E. White, Active metamorphism of upper Cenozoic sediments in the Salton Sea geothermal field and the Salton Trough, southeastern California, *Geol. Soc. Amer. Bull., 80,* 157-182, 1969.

Murray, K.S., J.W. Bell, B.M. Crowe,and D.G. Miller, Geologic structure of the Chocolate Mountain region, southeastern California, in *Geology and Mineral Wealth of the California Desert,* edited by D.L. Fife and A.R. Brown, pp.221-223, South Coast Geological Society, Santa Ana, Calif., 1980.

Nicholson, C., L. Seeber, P. Williams, and L.R. Sykes, Seismic evidence for conjugate slip and block rotation within the San Andreas fault system, southern California, *Tectonics, 5,* 629-648, 1986.

Okaya, D.A., Seismic profiling of the lower crust: Dixie Valley, Nevada, in *Reflection Seismology: The Continental Crust,* Geodynamics Series Volume 14, pp.269-279, AGU, Washington, D.C., 1986.

Palmer, T.D., J.H. Howard, and D.P. Lande (Eds.), *Geothermal Development of the Salton Trough, California and Mexico,* 45 pp, UCRL-51926, Lawrence Livermore National Laboratory, Livermore, Calif., 1975.

Robinson, P.T., W.A. Elders, and L.J.P. Muffler, Quaternary volcanism in the Salton Sea geothermal field, Imperial Valley, *Geol. Soc. Amer. Bull., 87,* 347-360, 1976.

Ron, H., R. Freund, Z. Garfunkel, and A. Nur, Block rotation by strike-slip faulting: Structural and paleomagnetic evidence, *J. Geophys. Res., 89,* 6256-6270, 1984.

Sharp, R.V., San Jacinto fault zone in the Peninsular Ranges of southern California, I. Geol. Soc. Amer. Bull., 78, 705-730, 1967.

Sharp, R.V., Tectonic setting of the Salton Trough, *U.S. Geol. Surv. Prof. Pap., 787,* 3-15, 1972.

Sharp, R.V., Some characteristics of the eastern Peninsular ranges mylonite zone, *U.S. Geol. Surv. Open File Rep., 79-1239,* 1-595, 1979.

Sharp, R.V., Tectonic setting of the Imperial Valley region, *U.S. Geol. Surv. Prof. Pap., 1254,* 5-14, 1982.

Sharp, R.V., M.J. Rymer, and J.J. Lienkaemper, Surface displacement on the Imperial and Superstition Hills Faults triggered by the Westmorland, California, earthquake of 26 April 1981, *Bull. Seismol. Soc. Am., 76,* 949-965, 1986.

Smith, R.S.U., W. Yeend, J.C. Dohrenwend, and D.D. Gese, Mineral resources of the North Algodones Dunes Wilderness Study Area, (CDCA-360), Imperial County, California, *U.S. Geol. Surv. Open File Rep., 84-630,* 1-11, 1984.

Sylvester, A.G., and M. Bonkowski, Basement rocks of the Salton Trough region, in *Tectonics of the Juncture Between the San Andreas Fault System and the Salton Trough, Southeastern California,* edited by J.C. Crowell and A.G. Sylvester, pp. 65-75, Department of Geological Sciences, University of California, Santa Barbara, Calif., 1979.

Terres, R. and J.C. Crowell, Plate tectonic framework of the San Andreas-Salton Trough juncture, in *Tectonics of the Juncture Between the San Andreas Fault System and the Salton Trough, Southeastern California,* edited by J.C. Crowell and A.G. Sylvester, pp. 15-25, Department of Geological Sciences, University of California, Santa Barbara, Calif., 1979.

van de Kamp, P.C., J.H. Howard, and A.N. Graf, Section 1: Geology, in *Geothermal Resources and Reservoir Investigations of U.S. Bureau of Reclamation Leaseholds at East Mesa, Imperial Valley, California,* Lawrence Berkeley Laboratory, LBL-7094, pp. 1-32, 1978

Vedder, J.G., D.G. Howell, and H. McLean, Stratigraphy, sedimentation, and tectonic accretion of exotic terranes, southern Coast Ranges, California, *Mem. Am. Assoc. Pet. Geol. 34,* 471-498, 1983.

Wallace, R.D., and D.J. English, Evaluation of possible detachment faulting west of the San Andreas, southern Santa Rosa Mountains, California, in *Mesozoic-Cenozoic Tectonic Evolution of the Colorado River Region, California, Arizona, and Nevada, Anderson-Hamilton Volume,* edited by E.G. Frost and D.L. Martin, pp. 502-510, Geological Society of America, Boulder, Colo., 1982.

White, D.E., and D.L. Williams, Assessment of geothermal resources of the U.S. - 1975, *U.S. Geol. Surv. Circ. 726,* 1-9 - 1-17, 1975.

Wilkinson, W.H., and C.J. Wendt, Precious metal mineralization, stratigraphy, and tectonics in southeastern California, in *Frontiers in Geology and Ore Deposits of Arizona and the Southwest,* edited by B. Beatty and P.A.K. Wilkinson, pp. 267-279, Arizona Geological Society Digest Volume XVI, Tucson, Arizona, 1986.

Winker, C.D., Neogene stratigraphy of the Fish Creek-Vallecito section, southern California: Implications for early history of the northern Gulf of California and Colorado delta, Ph.D. dissertation, 494 pp., University of Arizona, Tucson, 1987.

Younker, L.W., P.W. Kasameyer, and J.D. Tewhey, Geological, geophysical, and thermal characteristics of the Salton Sea geothermal field, California, *J. Volcanol. Geothermal Res., 12,* pp. 221-259, 1982.

Zoback, M.L., R.E. Anderson, and G.A Thompson, Cainozoic evolution of the state of stress and style of tectonism of the Basin and Range Province of the western United States, in *Extensional Tectonics Associated With Convergent Plate Boundaries* edited by F.J. Vine and A.G. Smith, pp. 407-434, Phil. Trans. R. Soc. London, Ser. A, 300, 1981.

C-1 MIGRATION

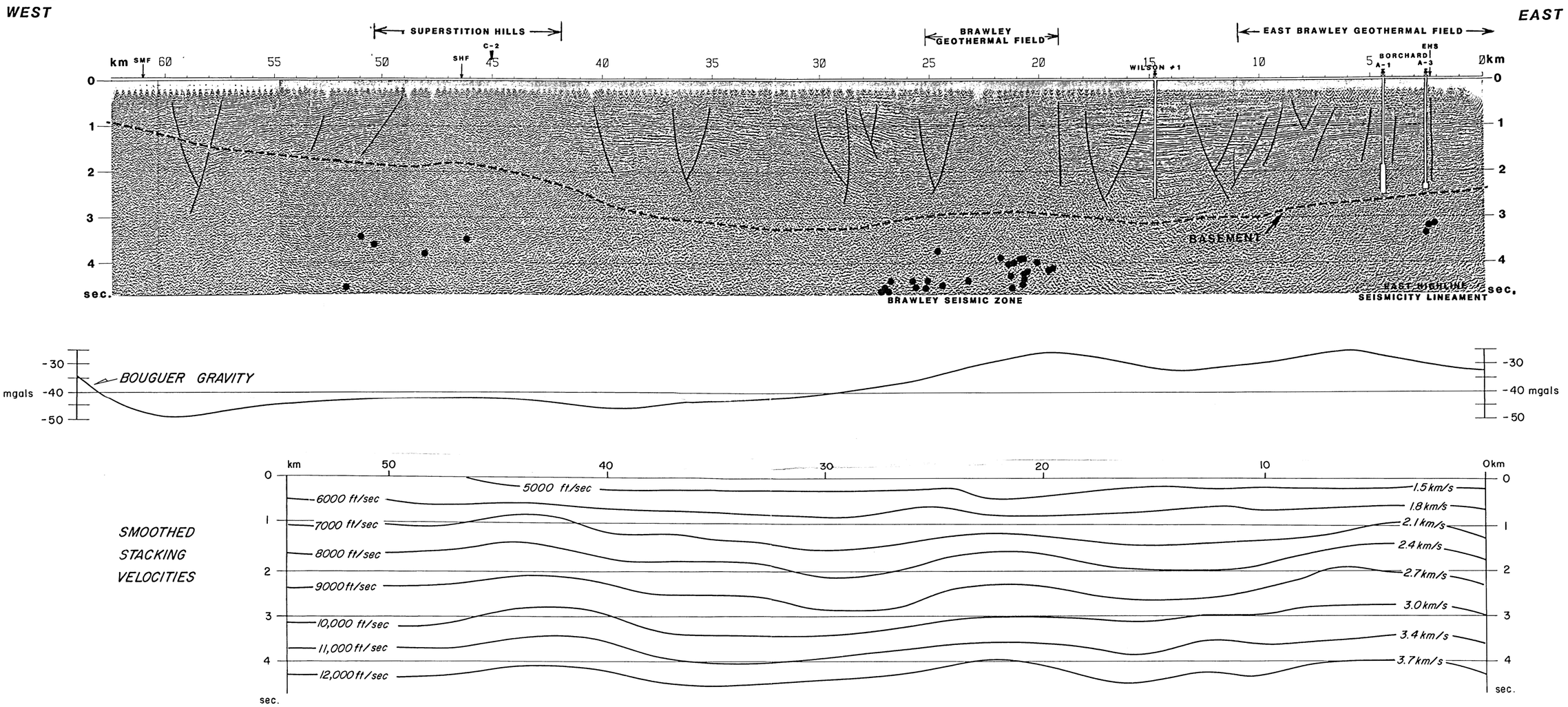

EHS = EAST HIGHLINE CANAL SEISMICITY LINEAMENT
BF = BRAWLEY FAULT
SHF = SUPERSTITION HILLS FAULT
SMF = SUPERSTITION MOUNTAIN FAULT

PLATE 1